Ngoc Tiep Nhu Nguyen

# Developing A Low-cost Myoelectric Prosthetic Hand

Metropolia University of Applied Sciences

Bachelor of Engineering

Electronics

Thesis

11 May 2018

| | |
|---|---|
| Author<br>Title<br><br>Number of Pages<br>Date | Ngoc Tiep Nhu Nguyen<br>Developing Low-cost Myoelectric Prosthetic Hand<br><br>47 pages + 2 appendices<br>18 May 2018 |
| Degree | Bachelor of Engineering |
| Degree Programme | Electronics |
| Professional Major | |
| Instructor(s) | Matti Fischer, Principal Lecturer |

The purpose of this Bachelor's study was to build a 3D printed prosthetic hand which can be controlled by an EMG signal from the forearm. For an amputee, upper limbs loss has many different consequences not only in terms of physically but also socially, economically and psychologically. The device aims to help the patients who have lost their hand due to accidents, diseases or birth defects with daily activities.

The device will be attached to the patient's forearm to replace the lost hand. A prototype prosthesis was created which has basic hand functionality. The prosthesis integrated DC and PWM motors, force sensors and myoelectric sensors. Three electrodes read the EMG signal will be attached in forearm to control the hand. There are five separate DC motors to controls each finger and one servo motor to control the rotation of the wrist. A touch sensor will be attached in the tips of prosthetic model's fingers to estimate the pressure that the prosthetic grip applies on the holding object. There will be a feedback loop from the touch sensor.

The final outcome is a complete prosthesis that met the initial design requirements and can perform basic hand functionality.

| | |
|---|---|
| Keywords | Electronics, Biomedical, EMG, Prosthetics hand |

# Contents

## List of Abbreviations

| | |
|---|---|
| EMG | Electromyography |
| SPI | Serial Peripheral Interface |
| MCU | Micro Controller Unit |
| PLA | Polylactic Acid |
| ABS | Acrylonitrile Butadiene Styrene |
| TEFLON | Polytetrafluoroenthylene |
| ADC | Analog to Digital Converter |
| IC | Integrated Circuit |
| MOSFET | Metal-Oxide-Semiconductor Field-Effect Transistor |
| LBI | Low Battery Indication |
| DC | Direct current |
| PCB | Printed Circuit Board |
| LED | Light Emitting Diode |

## 1 Introduction

Prosthetic hands are artificial devices designed for people with upper extremity amputations to provide them some functions of natural hands [1]. The number of amputation loss cases in the developing countries are significantly higher than in western countries due to lack of medical knowledge and the prevalence of illnesses that have been defeated in the developed world [2]. For an amputee, upper limbs loss has many different consequences not only in terms of physically but also socially, economically and psychologically. In order to minimize these consequences and assist the amputee to adapt to normal life, artificial hands and wrists are used to perform daily activities such as dressing, writing and grabbing different objects.

Nowadays, several commercial prosthetics devices are available. These devices' range varies from passive cosmetic hands to body harness power split-hooks, myoelectric hooks and hands. Despite all the different in their mechanical designs, control signal types and power sources, most of them are extremely expensive at hundreds or thousands of euros. Even cosmesses, prothesthetics made only for aesthetics, although less expensive, are still hundreds of euros. Therefore, in the developing countries only 5% of the amputees own a prosthesis not only because there are pricey, but also due to distribution and maintenance problems. One of the main purposes of this project is to develop a low-cost 3D printed prosthetic hand for patients in developing countries.

Figure 1 shows a typical myoelectric hand where surface electrodes on the amputee residual limb pick up myoelectric signals which are amplified and conditioned to allow the opening and closing of the hand.

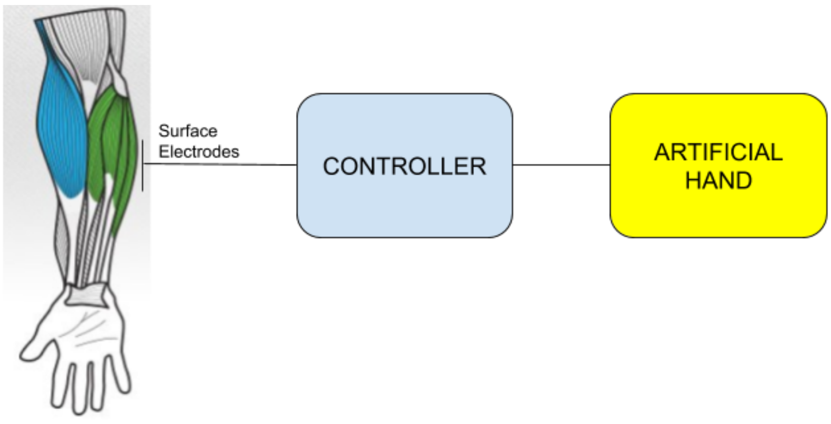


Figure 1: Myoelectric hand [3]

Innovations in 3D printing over the past decade, have made 3D printed transradial prosthetics an inexpensive alternative. They provide complex function at an affordable price. In the market, there are multiple designs that range very differently in ability and function such as durability, control system, hand grips, user inputs, comfort and cost. Each prosthetic design has its own strengths and weakness.

The purpose of this bachelor's study was to build a 3D printed prosthetic hand which can be controlled by an EMG signal from the forearm. The device will be attached to patient's forearm to replace the lost hand. Three electrodes reading the EMG signal will be attached in forearm to control the hand. There are five separate DC motors to controls each finger and one servo motor to control the rotation of the wrist. A touch sensor will be attached in the tips of prosthetic model's fingers to estimate the pressure that the prosthetic grip applies on the held object. There will be a feedback loop from the touch sensor.

The first and main task to be solved by conducting this research was to build a device in the form of a prosthetic hand which can be controlled by the patient. This aims at helping the patient perform simple daily tasks like grabbing and releasing objects. Since the device will be attached in the patient's forearm, the design needs to be light and the size needed to be suitable for this application. The second goal of the device is helping the patients to "feel" by the feedback signal from the touch sensor and vibration device in the forearm. The vibration intensity level will be indicated by the pressure which is read by the touch sensor. The third purpose of this project was to develop a low-cost prosthetic hand for patients in developing countries.

A prototype prosthesis was created that has basic hand functionality, a durable yet lightweight design utilizing 3D printing and a control unit, all available at a reasonable price point. The prototype was then evaluated against the required specifications. This report addresses the design process, manufacturing and testing of the 3D printed transradial prosthetic. This project collaborated with Reinis Geizans' thesis work on the "Developing 3D printed prosthetic hand model controlled by EMG signal from forearm". [4]

# 2 Background Research

## 2.1 Anatomy of Hand and Forearm

In order to create an appropriate artificial hand design, understanding the basic anatomy and physiology of the human hand is extremely necessary. Anatomy is the study of structure, and physiology is study of function. Through the study and understanding of the structure and function of the human hand, a better prosthesis model can be created.

The natural hand is in many ways a perfect instrument. It embodies multiple degrees of freedom and is capable of integrated function. With the current technology, it is unrealistic to think that all the criteria and performance specification of the normal hand could be reproduced in a man-made hand device [5]. However, it is possible to compromise from such ideal specifications and to design a realistic hand prosthesis. The main purpose of this part is to analyse the function ability of natural hand and to determine the hand's most common grasping patterns from an infinite variety of patterns.

### 2.1.1 Hand and Its Anatomical Plane

The hand consists of five digits: thumb, index finger, middle finger, ring finger and little finger. The hand's anatomy consists of 27 bones and over 20 joints, and it involves the use of over 33 different muscles [6]. Each factor plays a different role in the hand's functional activities. Bones are responsible for rigidity within a segment of a hand, joints provided that freedom of movement and muscles serve to move rigid segments on each other. Since a great part of hand prosthesis design is associated with the motion of the human hand and the range of motion of a human hand is restricted by the freedom of joints rather than activity of musculature [7], the study of bone and joint movement will help to determine the basic grasping patterns of the natural hand.

Defining the anatomical planes is necessary to analyze the motion of the hand (Figure 2). In figure 2-A, the limb segments' rotation is defined relative to the anatomical planes. Flexions and extension occur in the sagittal plane, abduction and adduction in the coronal plane, and external and internal rotation in the transverse plane. In Figure 2-B, the anatomical planes are shown in relation to the body in the standard position. In Figure 2-C, the plane of the palm is the coronal plane. The plane perpendicular to the coronal plane running the length of the hand is the sagittal plane, and the third plane, which is perpendicular to both the coronal and sagittal planes, is the transverse plane. In the resting or neutral position, the thumb sticks out from the palm and is not oriented with the anatomical axes.

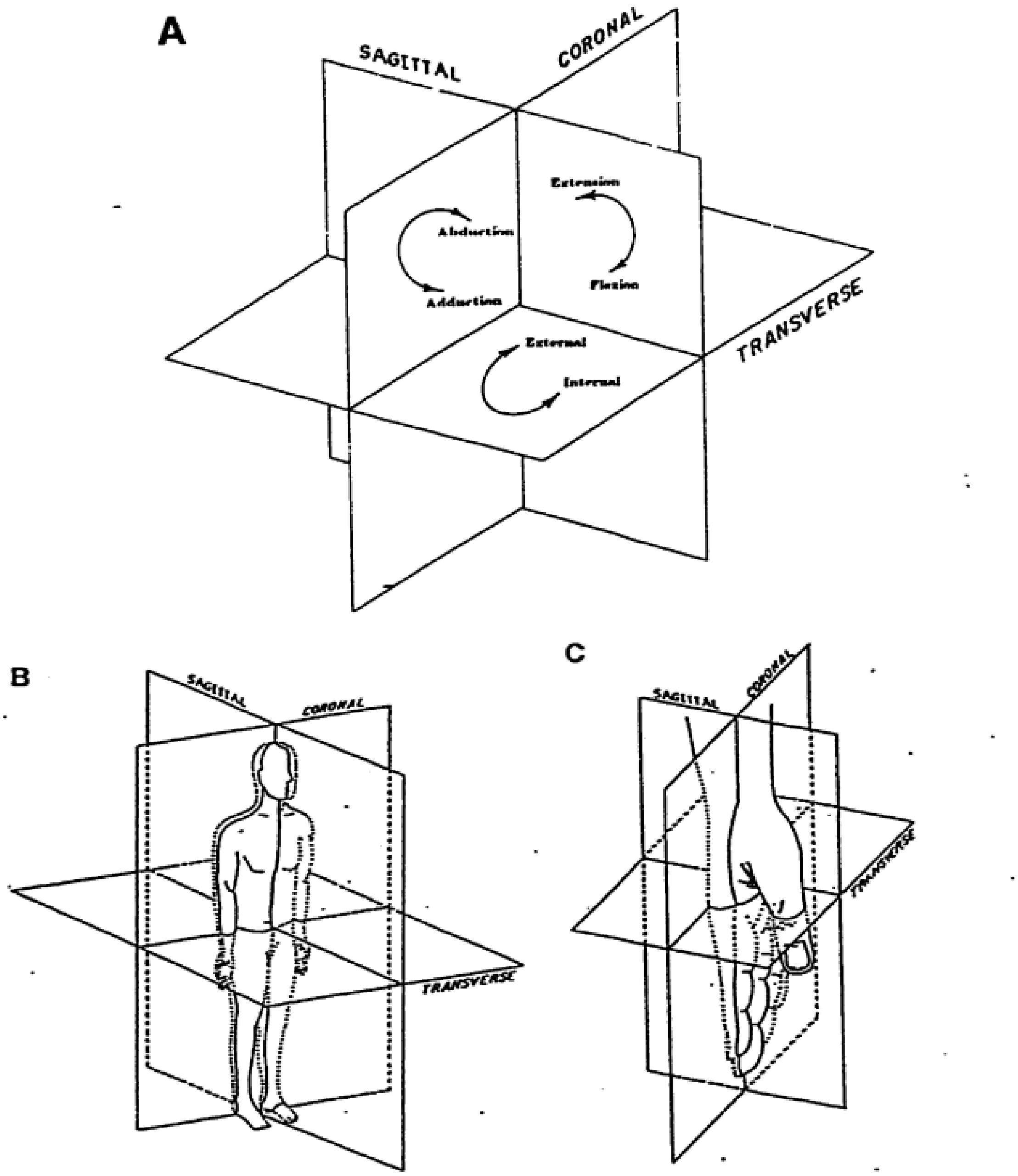


Figure 2: Anatomical planes [5] A) The rotations of the limb segments are defined relative to the anatomical planes; B) The anatomical planes are shown in the relation to the body in the standard position; C) The anatomical planes are shown in the relation to hand in the standard position.

### 2.1.2 Bones, Joints and Muscles of Hand

The bones of the natural hand, shown in Figure 3, naturally group themselves into the carpal bones, comprising of eight bones which make up the wrist and root of the hand, and the digits, each composed of it metacarpal and phalangeal segments [6]. The carpal bones are arranged in two rows, those in the more proximal row articulating with the radius and ulna. Between the two is the intercarpal articulation. The bony conformation and ligamentous attachments are such as to prevent both lateral and dorsal-volar (the palm of the hand) translations and also to allow participation in the major wrist motions. These are either wrist extension and flexion in the sagittal plane or abduction and adduction in the coronal plane.

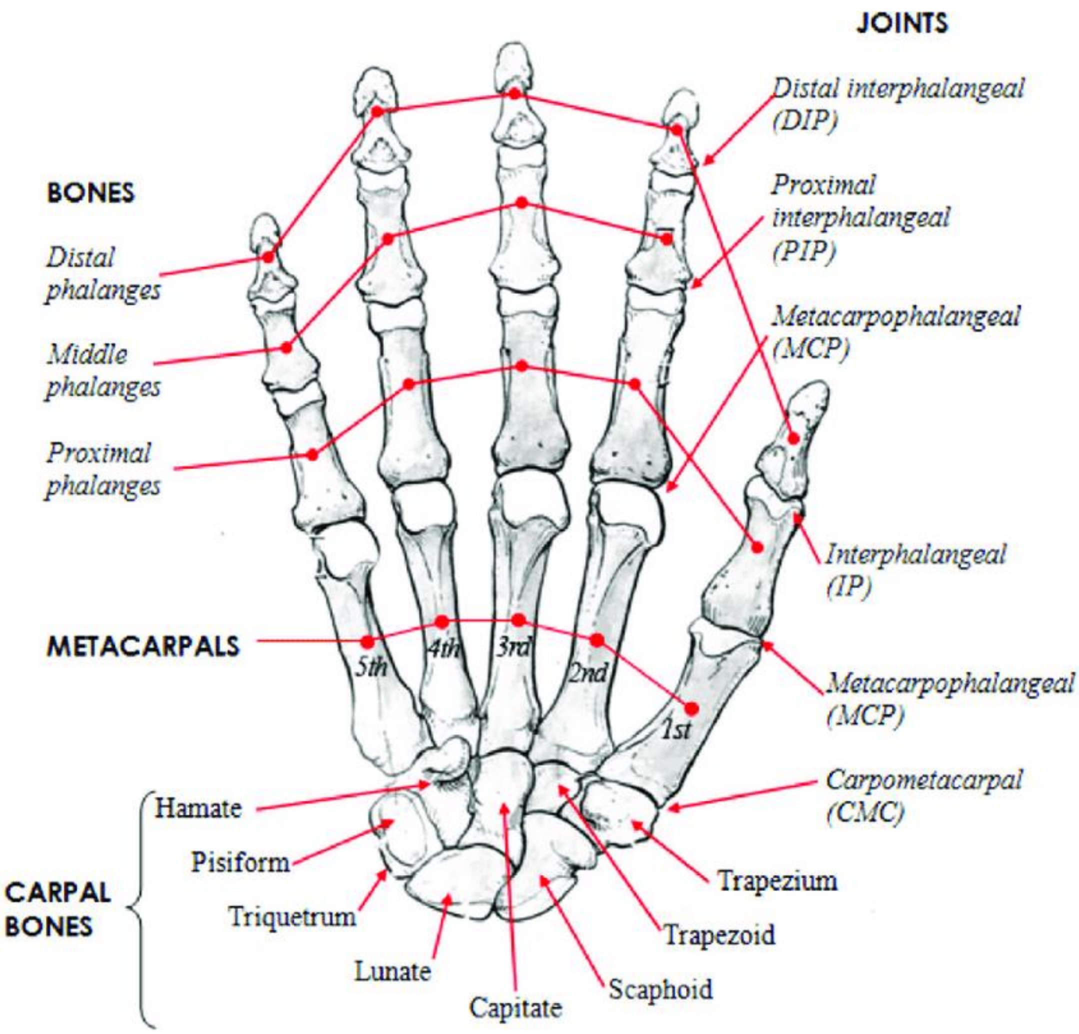


Figure 3: Bones and joints of the hand [8]

In each of the fingers, the anatomical design is essentially the same. Each finger consists of four bones (Figure 2): carpal, metacarpal and proximal, middle and distal phalanges.

The carpometacarpal (CMC) joints of the fingers are gliding joints and virtually immovable. The metacarpal joints are condyloid joints which allows for motion about two axes. In the sagittal plane, the flexion/extension motion range is about 90 degrees and in the coronal plane, the abduction/adduction is 20 to 40 degrees. The proximal and distal interphalangeal joints are single axis hinge joints which are capable of allowing flexion/extension through 90 degrees.

Intrinsic and extrinsic are the two group of muscles that comprise the hand and wrist. Fingers can move precisely and independently thank to intrinsic muscles. There are four different group of intrinsic muscles: the thenar muscles, that act on the thumb; the hypothenar muscles, that act on the little finger; the lumbrical muscles that help the extension of the Interphalangeal (IP) joints and the flexion of the Metacarpophalangeal (MCP) joints; and the interossei help the abduction and adduction of the fingers as shown in Figure 4

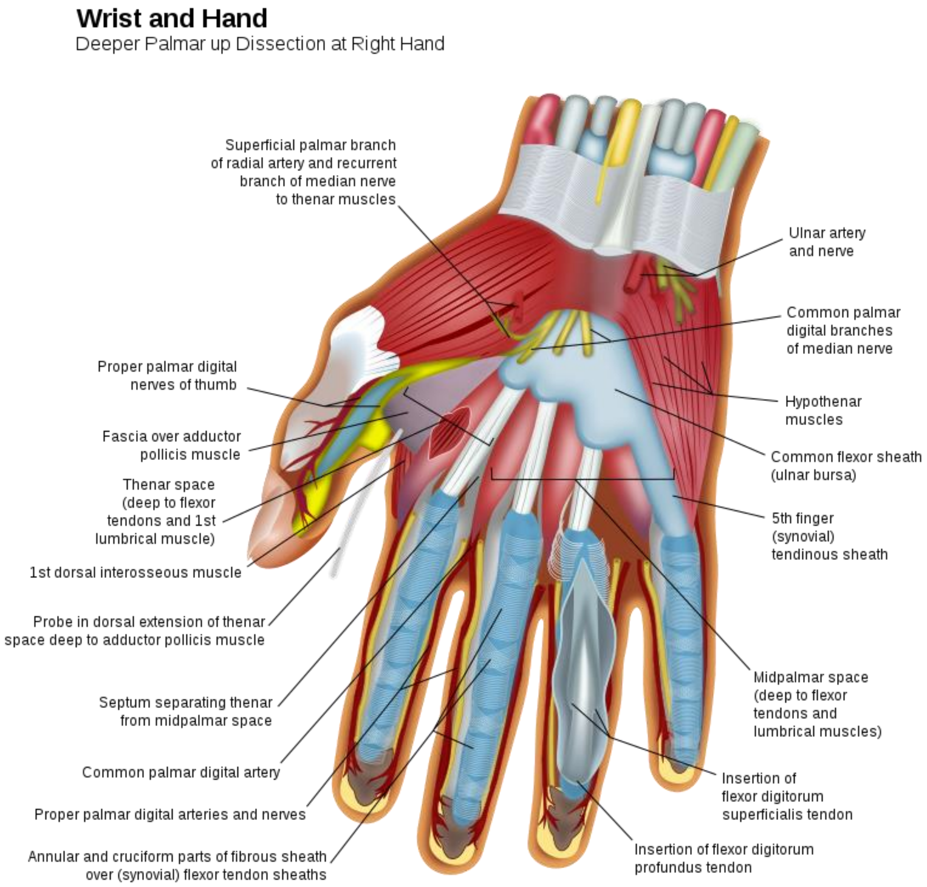


Figure 4: Muscles of hand [9]

### 2.1.3 Forearm Muscles

The superficial layer of the posterior forearm consists of seven muscles (Figure 5A): Brachioradialis, Extensor carpi radialis longus and brevis, extensor digitorum, extensor digit minimi, extensor carpi ulnaris and anconeus. The anterior forearm superficial layer has four different muscles (Figure 5B): Flexor carpi ulnaris, palmaris longus, flexor carpi radialis and pronator teres.

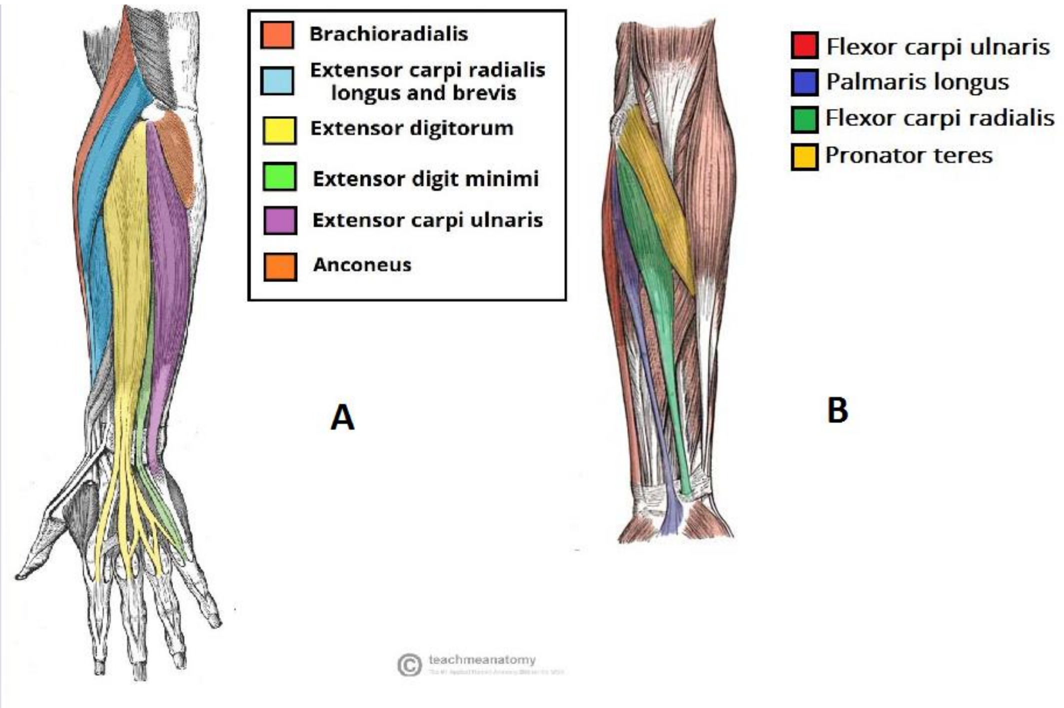


Figure 5: The muscles in the superficial of [10] A) The posterior forearm B) The anterior forearm

As shown in figure 6, natural fingers and thumb have no muscles. All the muscles that control the fingers are located in the palm and forearm. These muscles connect to the finger via tendons. The muscles that help to control the hand start at elbow or forearm running down to cross the wrist and hand. Few of these muscles position and steady the wrist and hands while some others help to allow the thumb and fingers to grab things and perform as a motor function. As shown in figure 6, the main muscles that move the finger up and down are flexor digitorum and extensor digitorum and the interossi muscle in the hand allow fingers to move side to side.

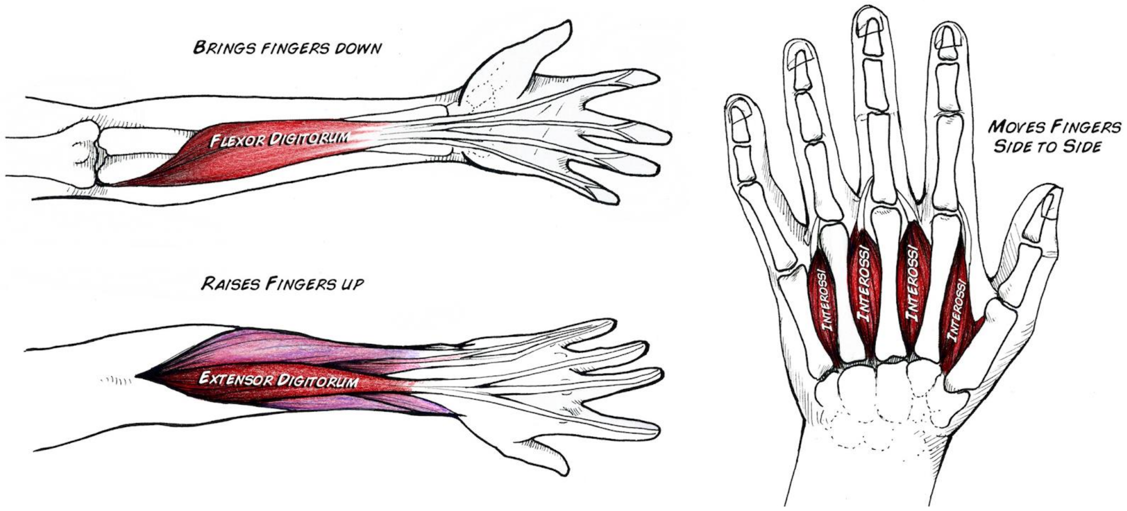


Figure 6: The group of muscles that control fingers [11]

## 2.2 Current Technology

Nowadays, there are many different commercial transradial prosthesis available and also many of prosthesis hand products under development. This section will mention, evaluate and analyze few available innovative designs in the current market.

### 2.2.1 Rehabilitative Robotic Glove

The Rehabilitative Robotic Glove (figure 7) is the proof of using durable string-base actuation concept. The glove was designed by AIM laboratory of Worcester Polytechnic Institute which was meant to aid the rehabilitation of those who had recently undergone a stroke. According to AIM laboratory report the gloves utilize a cable system to open and close a patient’s hand and servomotors actuate the cables. The research group has chosen Kevlar k49 cables due to their tensile strength and low elasticity. Cables are placed on each side of finger and attached to a servo and spool. As a result of this design, based on which direction the servos move the gloves always pulls the fingers to a desired position. [12].


Figure 7: Rehabilitative Robotic Glove [12]

### 2.2.2 Bebionic Hand

Bebionic hand (Figure 8) was designed by Ottobock, a German tech company. So far, the Bebionic artificial hand is one of the most lifelike, functional and easy to use myoelectric hand commercially in the world. This prosthetic hand not only can offer 14 different grip patterns but also various wrist options such as quick disconnect, multi-flex, flexion and short wrist. The company also developed a built-in sensor to allow the user to have selectable thumb position. Bebionic hand can handle up to 45 kilos due to its durable construction and advanced materials. The patients can confidently use this artificial hand to carry heavy objects or push themselves up from a seats position. [13]


Figure 8: Bebionic hand [13]

### 2.2.3 e-NABLE's Limbitless Arm

e-NABLE is a community for all the individuals from all over the world who use 3D printers to create 3D printed hands or arms for the ones in need of an artificial upper limb. The community was founded in 2013 and so far they has provided over two thousand designs for those who are in need of a prosthetic arm. At the moment, most of the designs are mechanically powered by a functional wrist or elbow. e-NABLE's first myoelectric design is Limbitless Arm which is an open-source design featuring an Arduino Micro microcontroller, a single servo capable of producing torque, muscle sensors, and Kelvar survival cord to move the fingers. The most disadvantaged feature of this design is that because there is only a single servo motor in the design, the hand can only open and close. On the other hand, the limbitless arm is very inexpensive and comfortable for the user [14]. Figure 9 shows the Limbitless Arm.

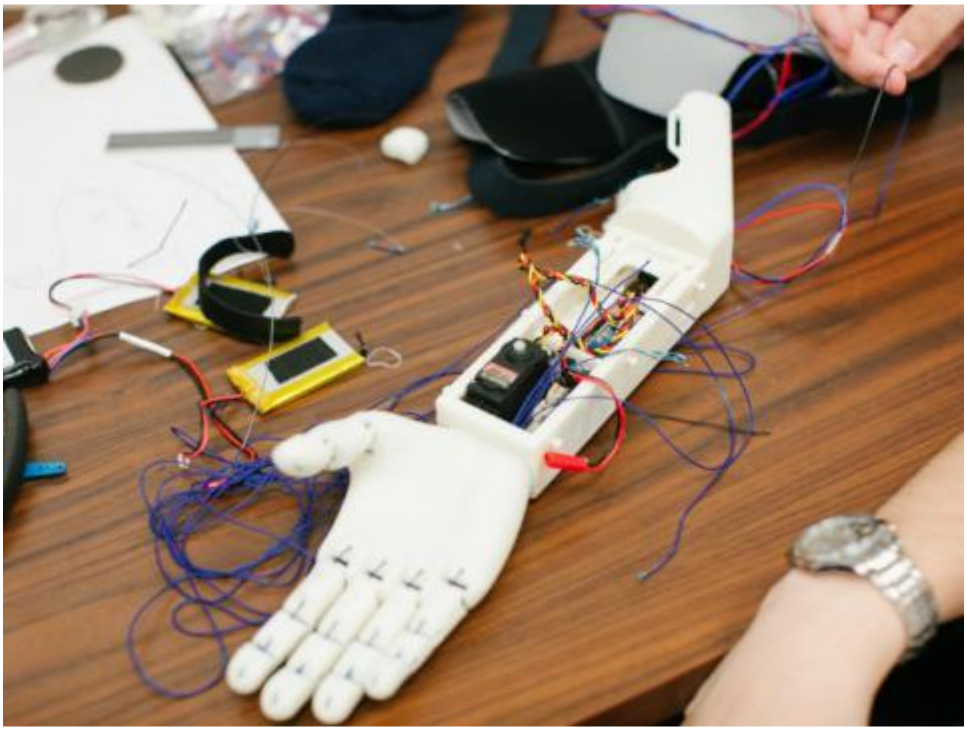

Figure 9: Limbitless Arm [14]

## 2.3 Electrical Signals from Muscle – EMG (Electromyogram)

An EMG signal is the graphical representation of the electrical activity of muscles. Myoelectric refers to the electrical properties of muscles. When somebody thinks about flexing a muscle, their brain sends a neuromuscular or electrical signal to the muscles. At this moment, the muscles start using motor units, or bundles of muscle fibers which generate forces behind the muscles. The harder the muscle is flexed, the more motor units are recruited to generate greater muscle force and the greater the number of motor units, the more electrical activity the muscle produces. [15]

The amplitude of an EMG signal ranges from 0 to 10 mV and dominant energy is limited to the 0 to 500 Hz frequency range. There are two common ways to detected myoelectric signal: at the skin surface using non-invasive surface electrode, or more invasively from within the muscle belly using needle fine wire, or implanted electrode. The non-invasive method usually picks up significantly amount of noise from both external and internal sources. There are three main noise sources for EMG signals: Inherent noise, Ambient noise and Motion artifacts.

Inherent noise: All the electronics components that are used to detect and record the EMG signals generate electrical noise. The noise from electronics components can range from 0 Hz to several kHz. This noise cannot be eliminated and can only be reduced by using high quality electronics components, good circuit design and construction techniques.

Ambient noise: This noise comes from electromagnetic radiation devices such as radio, television transmission, electrical wire etc. The dominant concern for the ambient noise arises from the 50 Hz radiation from power sources.

Motion artifacts: The interfacing layer between the detection surface of the electrode and the skin and the movement of the cable connecting the electrode to the amplifier are the two-main noise source of motion artifact. These two-noise source have a frequency range from 0 to 20 Hz.

Nowadays, myoelectric control using pattern recognition has involved many different methods for feature extraction and classification of myoelectric data. Feature extraction has different methods such as spectral power magnitude values, autocorrelation, cross-correlation values, Hudgins' feature set, autoregressive coefficients and time-domain statistics etc. For the classifiers, there are various methods such as artificial neural networks, fuzzy systems, linear discriminant analysis and Gaussian mixture models.[15]

# 3 Mechanical Design of Prosthetic Hand

## 3.1 Overview and Open Source Model Design

For this project, using open source hand model option was chosen to save time and the emphasis of this project is on electronics design and embedded system coding, not on 3D modeling. There are many different 3D printed open source prosthetic hands available in the internet. After reviewing all the pros and cons aspects of many available models, the palm design which is called “Flexy Hand 2” which was designed by Steve Wood was chosen [16]. The full design description and detail are explained in Appendix 1.

Steve Wood, the designer of the hand, has declared that he created the hand to be used one day as a prosthetic device. His first design (Figure 10-A) was not a functioning prosthetic hand; its fingers could be only manipulated by pulling cables attached at the wrist. After that, Wood decided to start designing the second iteration of the “Flexy-Hand”. He has adapted the concept of the first “Flexy-Hand” and create “Flexy-Hand 2” (Figure 10 - B) that could be put onto a human being’s arm and function like a real hand.[17]

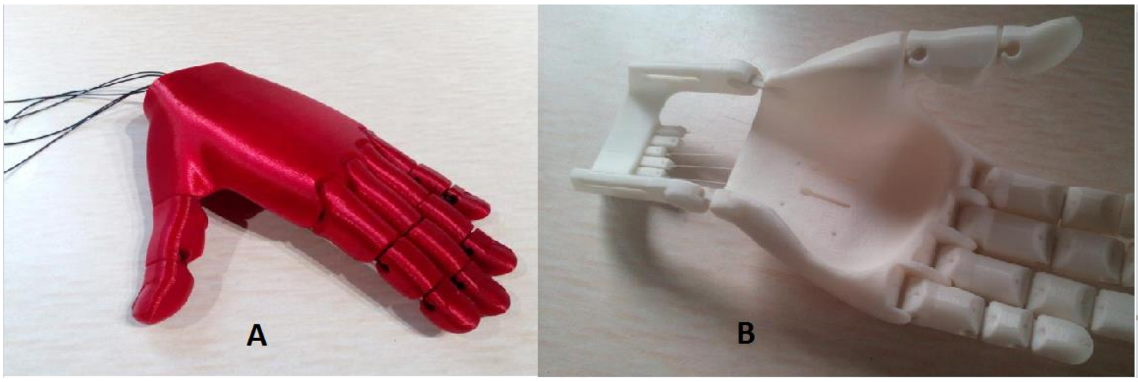


Figure 10: 3D printed hand model created by Steve Wood [15] - A) Flexy Hand version B) Flexy hand version 2 [16]

According the Steve Wood, the majority of the “Flexy Hand 2” is 3D printed. However, to make it fully functional, it does consist of a few additional pieces such as the tendon cord, M2 screws (used as tensioners), Velcro style straps etc. Figure 11 shows the 3D design model of “Flexy Hand 2”

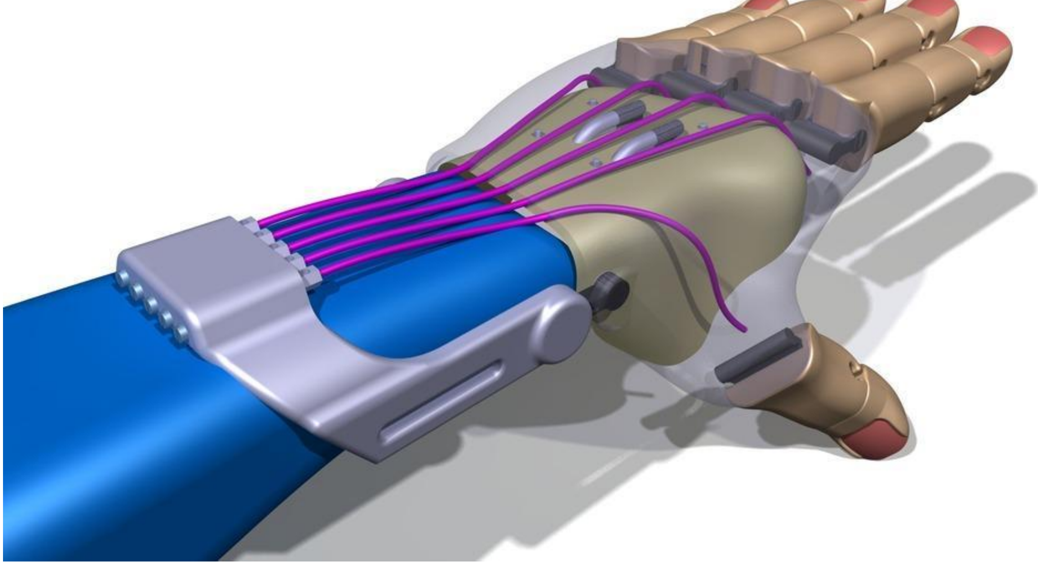

Figure 11: “Flexy Hand 2” 3D model design [17]

Out of many available hand models on the open source website, this hand model was chosen because it represents the human hand anatomy most accurately. In addition, this hand model fixes perfectly the project’s purpose which is free movement between individual fingers. However, to be applied for this project, the hand design needs to be considerably modified and adapted to many different features. The original “Flexy Hand 2” model is meant for mechanical actuation, it is actuated by springs and strings; therefore, to achieve finger closing action it is necessary to bend the wrist itself. Bending the wrist will close the finger at the same time, making bonded wrist and fingers.

For this project, it is necessary to design a new attachment to the patients’ upper hand which is called the stump and this part has to include a PWM motor to control wrist, printed circuit board, wires and batteries. In reality, every patient has a unique physiology of the stump and a unique gauntlet design should be made for each individual patient. This would be a challenge for this project to scale up in the future; however, with inexpensive 3D printing technology it is possible to print new prosthetics and gauntlets every few months, this feature will be especially useful for kids. Figure 12 shows the new 3D design of the gauntlet for this project.

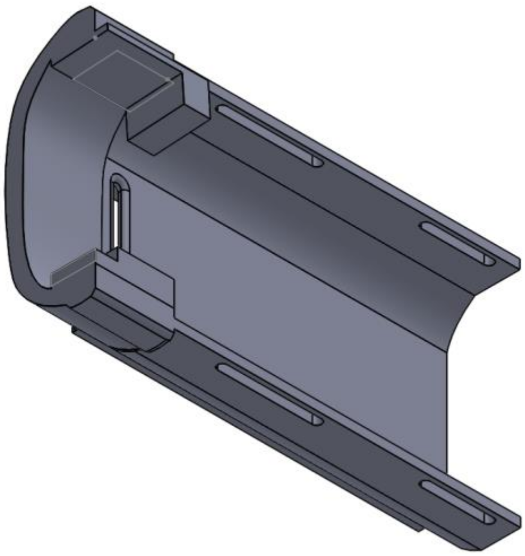

Figure 12: The new gauntlet design

For this project, “Finder” 3D printer by Flashforge Cooperation was used to create the mechanic part of the artificial hand. Flashforge provides a 3D printed software which is named “Flash Print” for users to design and review printed part. One of the best features of “Flash Print” is allowing user to choose the internal structure of printed part, this is achieved by creating honey comb filling in the parts that would be either completely hollow or solid. Printing a completely solid part would make them very rigid by also much heavier. Honey comb was used for the internal structure to reduce the part’s weight (figure 13)

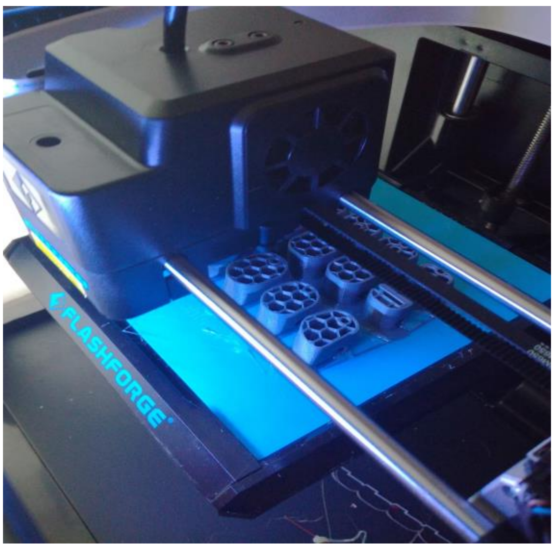


Figure 13: 3D printing fingers with honey comb inserts

“Finder” 3D printer allows the use of different materials such as PLA (Polylactic acid), ABS (Acrylonitrile Butadiene Styrene), TEFLON (Polytetrafluoroethylene) and many more. Different plastics with different additives will have different properties. For this specific project, the main printing material is PLA plastic due to environmental reasons. Unlike other thermoplastic polymers, PLA is derived from renewable resources like corn starch or sugar cane; therefore, it is extremely environmentally friendly. However, because the PLA plastic is usually very rigid, this material is not suitable for printing the joint part which needs to be bendable and flexible. For the joints to connect between different parts of the fingers, another special filament was chosen. The special flexible filament was bought from Velleman Oy in Finland. Unfortunately, the manufacturer has not provided any specification of the polymer used to produce this elastic 3D printer filament. [18].

## 3.2 Mechanics Modifitcation

Other than the modification of the gauntlets to suit the design with every individual users, there are many other mechanics that needed to be modified such as finger actuator servo motor, continuous rotation, servo motor etc.

### 3.2.1 Finger Actuator Servo Motor Modification

For finger actuation, a SG90 servo motor was chosen. This small and simple motor was chosen since it can provide the necessary features such as small size, light weight, integrated gearbox and cheap price. Figure 14 shows the picture of SG90 servo motor [18].


Figure 14: SG90 servo motor [19]

Despite all the advantages, this servo motor also has some limitations that were necessary to modify. SG90 are originally designed for a specific degree rotation, in this case it is 180 degrees and 90 degrees in each direction. This feature was caused by the hardware limit in gearbox and feedback potentiometer. In this project, the servo motors need to have continuous rotation and continuous rotation feedback loop.

To achieve the continuous rotation, the servo motor was completely disassembled, and some modifications were performed with the gearbox such as removing the physical stop wedge from the gear and potentiometer. The gear has half shaft hole that is attached to potentiometer to provide a feedback signal. This hole was drilled to full circular hole. The purpose of this modification is to disengage gear rom the potentiometer feedback shaft and removed wedge allow full uninterrupted continuous rotation by keeping all original gearbox parts. Figure 15 shows the gearbox before and after modification.


Figure 15: Gearbox before (A) and after (B) modification.

### 3.2.2 Servo Arm Replacement:

The servo motor has an attachable arm on an output shaft from the gearbox, this arm is shown in Figure 15-A. It provides the possibility to attach the servo motor to the different attachments. However, in this case the arm’s swing has large radius and is not only suitable for compact design but also a swing arc is not long enough to close the artificial hand’s fingers completely. Therefore, the servo arms were replaced with 3D printing pulleys. Moreover, the actuator string will be winded on pulley allowing hand to close and hold different objects in tighter grip. Figure 16 shows the modification servo motor which has been attached a new pulley and removed the potentiometer. In addition, there was a servo driver integrated circuit board still visible which was removed later on.

Figure 16: The modification servo motor

In the final assembly, there has been one addon to the modified servo motor, this addon is coupling shaft from the pulley to the rotary encoder. Figure 17 shows the test fitting motor assembled in the hand and the finished modification servo motor.

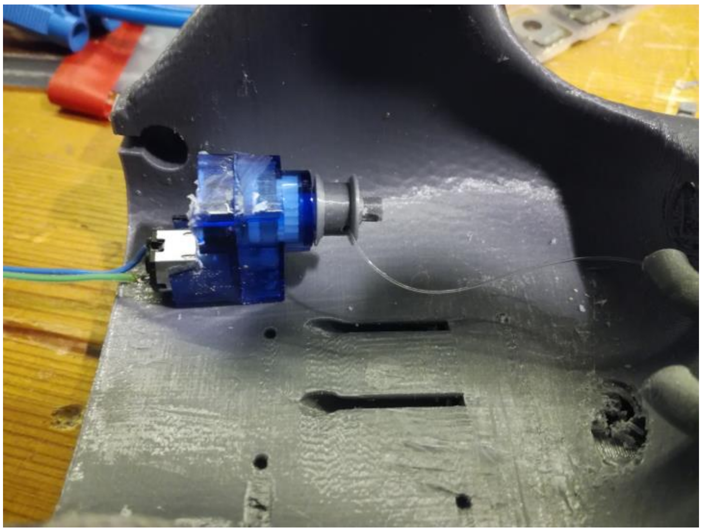

Figure 17: Fitting the servo motor in the hand's palm.

## 3.3 Hand Assembly

The mechanics assembling process started with the fingers part. The fingers are assembled by sliding flexible joint pieces in part which is replacing the Phalanx bones of the artificial hand. Figure 18 demonstrates the finger assembling procedure. As shown in figure 18-B, the white pieces represent the flexible joints of the hand. These pieces not only function as hinges but also help the fingers to return to the original or adduction position after the tension on the string of that finger has released.

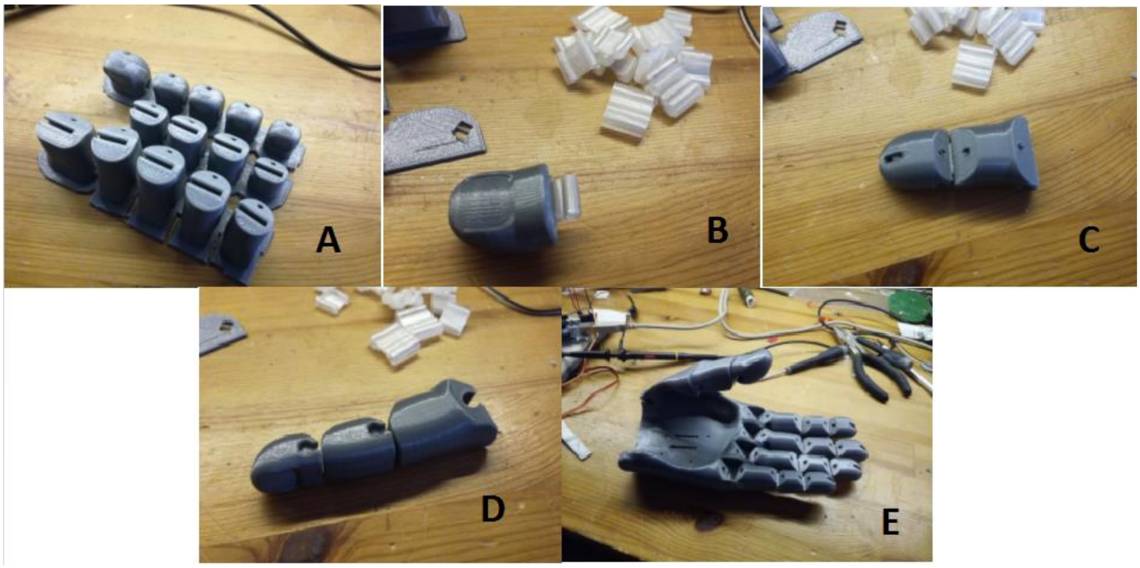


Figure 18: Hand mechanics assembling procedure. A)3D printed Phalanx bones B) Sliding joint in the first Phalanx C) Sliding joint in the second Phalanx D) Sliding joint in the third Phalanx E) The final assembled hand without motors

The original model wrist assembly follows same procedure, which is using flexible joint pieces to attach hand to the gauntlet. For the new gauntlet that includes a wrist actuator motor it is necessary to have solid a hinge mechanism. All parts have been 3D printed and attached to gauntlet. Figure 19 demonstrate the hand and gauntlet assemble with the PWM motor.

Figure 19: Hand and gauntlet assemble with PWM motor

Additionally, some smaller parts for the hand and gauntlet were printed and attached to the base material, for example, a 90-degree guide pipe to align the string to pulley mechanism. Need for these extra parts were discovered in the assembly process of the prototype prosthesis, in the final product these modifications would be included in a single-piece printable model. Figure 20 - A and B illustrate the hand with finger actuator motor and guide pipes and final test fitting the finger actuator respectively. As shown in figure 20-B, the pulley mechanisms together with the guide pipes and the feedback rotary encoder.

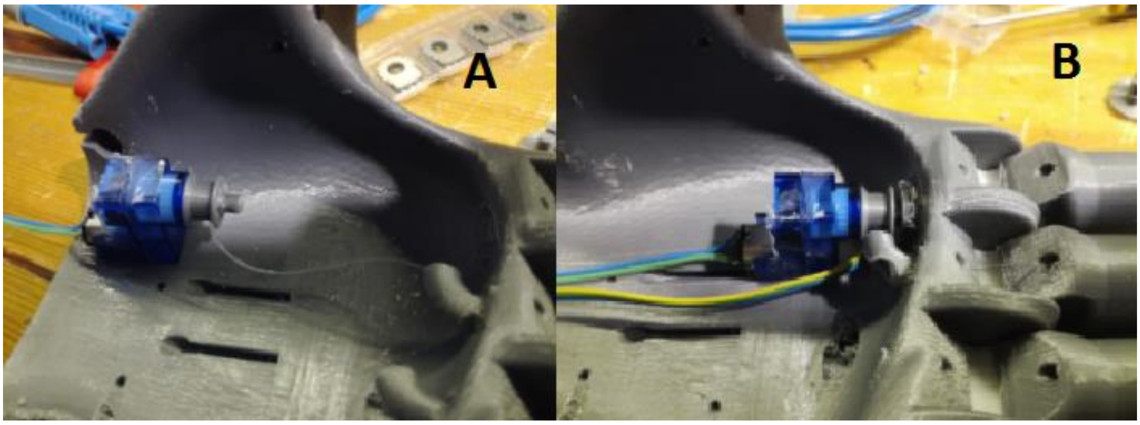


Figure 20: Finger actuator motor assemble A) Hand with finger actuator motor and guide pipes B) Finger actuator final fitting test

Figure 21 shows the completed assembled mechanical part of the prosthetic hand.

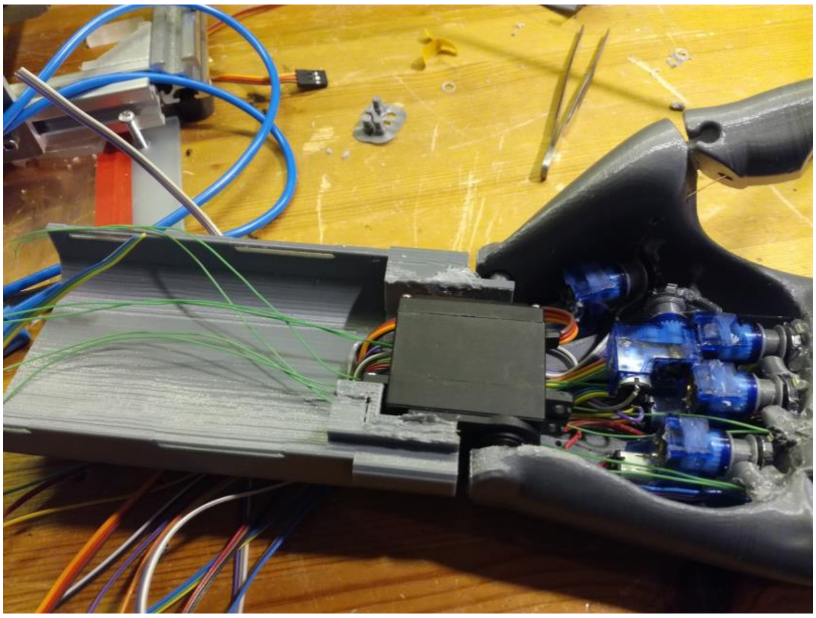

Figure 21: The completed assembled mechanical part of the prosthetic hand.

# 4 Schematic and PCB Design

Instead of designing electronics circuit from discrete components, integrated circuit was chosen to be used for this project. There are many different reasons that can be explained for this decision. First of all, the modern IC (integrated circuit) allows for inexpensive and small footprint design with more feature compared to designing circuit from discrete components. Smaller number of external components has benefits of lowering overall cost of the product. Secondly, using IC makes PCB (printed circuit board) design more simple and takes up a smaller footprint. Finally, IC provides many different including features than the option designing circuit for discrete components. Having extra feature of circuit besides its intended main function without adding any extra components is extremely beneficial for the price and size of the final product. One the strong example for the extra feature of IC is the battery low voltage cut off circuit, if we look at the battery charging circuit which is mentioned in 4.4 section, using IC allows to add many of extra safety feature without adding any extra components.

## 4.1 Overall Electronic Design Block Diagram

This section explains about the overall block diagram of this project electronics design. Block diagrams are used to understand and design complete circuits by dividing them down into smaller sections or blocks. Each blocks of the diagram perform a particular function and the block diagram shows how they are connected together [20]. Figure 22 illustrates the overall block diagram of the circuit. As show in the figure, the design is divided into three main parts: electronics circuit on the PCB, on the hand and the others external devices/power input.

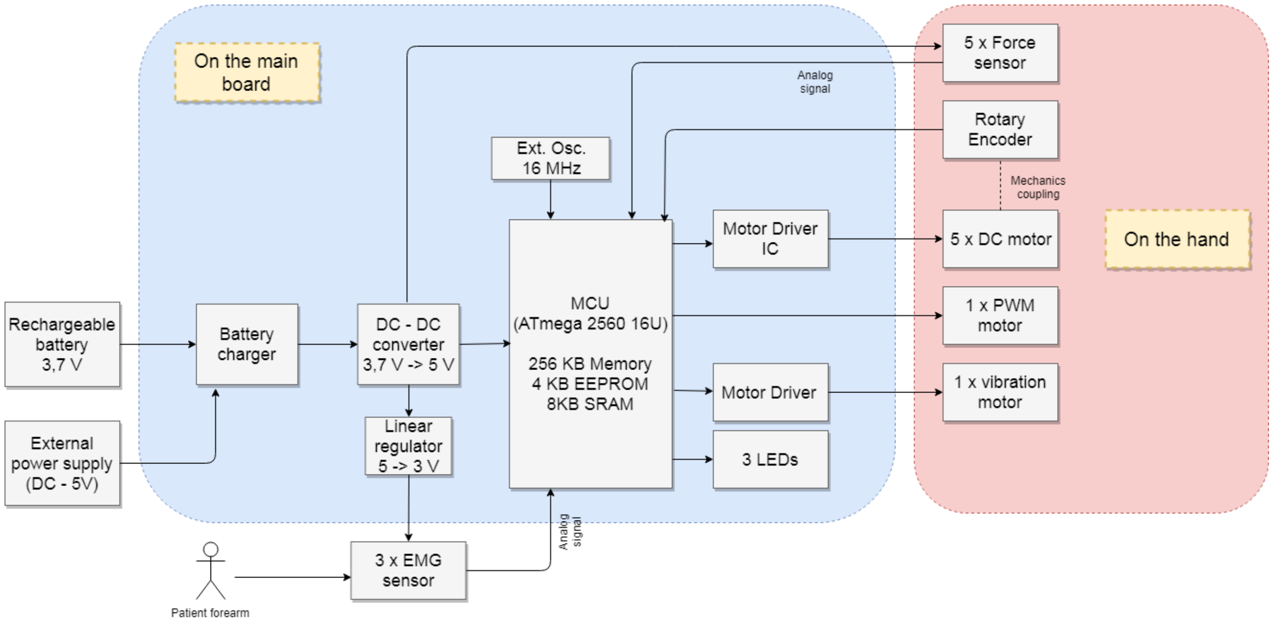


Figure 22: Electronics circuit block diagram

In figure 22, the part in blue square is on the PCB circuit. These parts are electronics components that do not have mechanical functionality. The light pink square includes the parts that are attached straight on the 3D printed hand, these components have mechanical function. According the diagram, the EMG sensors are located outside of the main PCB and attached to the user's forearm. These sensors send analog signal to microcontroller and are connected with main board via wires. The main reason for not integrating EMG sensors in the prosthesis gauntlet is that it is mandatory to attached on the forearm and located in the right muscles position to collect EMG signal.

For this project, the rechargeable battery is outside of main PCB due to two main reasons such as easy replacement and weight distribution. Placing the battery outside of the main PCB not only allows the user to easily replace it without damaging the device but also making it possible to swap the original battery with bigger capacity ones. In addition, batteries are relatively heavy components, especially with high capacity ones. Providing the user, the capability to place the battery anywhere for example on bicep helps with the weight distribution and increasing the comfortability for the user. The full schematics design is attached in Appendix 2.

## 4.2 EMG Sensors Circuit

Out of many different EMG sensors available on the market, MyoWare Muscle Sensor (AT-04-001) which is manufactured by Advancer Technologies company was chosen for this specific project. MyoWare sensor is a module type circuit. This sensor consists of biomedical sensor pads, integrated circuit and PCB board. Is has been designed as a wearable device meaning it is designed to place on body directly as biomedical sensor pads are attached directly to PCB board instead of using biomedical pads separately and connecting them via wires [21]. Figure 23 shows the Myoware Muscle Sensors and table 1 gives the electrical specification of the sensor.

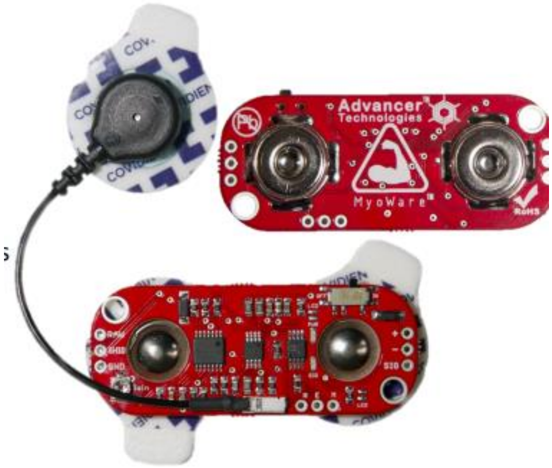


Figure 23: MyoWare Muscle Sensor [21]

Table 1: Electrical Specification of MyoWare Sensor [21]

| Parameter | Min | Typical | Max |
|---|---|---|---|
| Supply Voltage | +2.9 V | +3.3 or +5 V | +5.7 V |
| Adjustable Gain Potentiometer | 0.01Ω | 50 kΩ | 100 kΩ |
| Output Signal Voltage<br>EMG Envelope<br>Raw EMG (centered about +Vs/2) | <br>0 V<br>0 V | <br>--<br>-- | <br>+Vs<br>+Vs |
| Input Impedance | -- | 110 GΩ | -- |
| Supply Current | -- | 9 mA | 14 mA |
| Common Mode Rejection Ratio (CMRR) | -- | 110 | -- |
| Input Bias | -- | 1 pA | -- |

The MyoWare Muscle Sensor is a prefabricated PCB that contains the necessary hardware to translate small variations in voltage in a muscle into analog values that can then be read by a microcontroller. The MyoWare Muscle sensors' signals are collected from the electrodes that are directly attached with the user's skin. In the current market, there are many different types of electrodes; however, this device will focus on multi-purpose medical electrodes and conductive fabric. To have a good control of the prosthetic hand, it is best that the electrodes receive a strong, clear signal. In reality there are various ways to achieve it such as maintaining skin-to-surface contact, receiving minimal noise and interference, and having a high conductivity.

There are three MyoWare sensors in the device which two of them are placed on the flexor muscle of the forearm and one on the bicep. Figure 24 shows that Myoware Muscle Sensor has nine pins in general: power supply (+Vs), ground (GND), output signal (SIG), Mid Muscle Electrode Pin, End Muscle Electrode Pin, Reference Electrode Pin, Raw EMG Signal and Shield Power

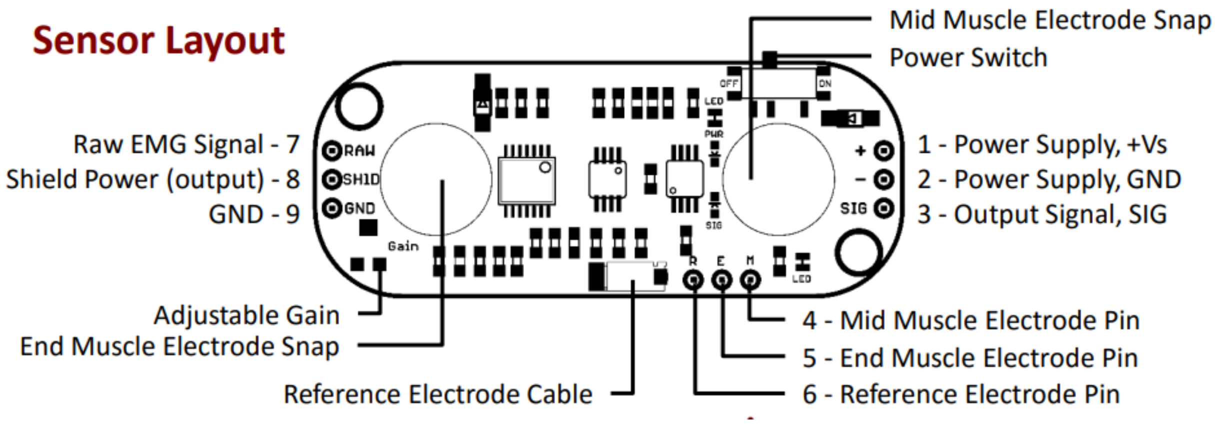


Figure 24: MyoWare Muscle Sensor layout [22]

Although the MyoWare Muscle Sensor offers reconfigure for Raw EMG Output and connecting external electrode cables option, this project uses the signal out from Output signal pin 3 (SIG) and electrode pads are attached straight to Mid and End muscle electrode snaps on the MyoWare Muscle Sensors' PCB board.

The schematic in figure 25 shows that there are in total 12-pin configuration for the myoelectric sensor. Four pins are used as power, four are used as ground, and ADC0 to ADC3 are the respective analog output of each sensor.

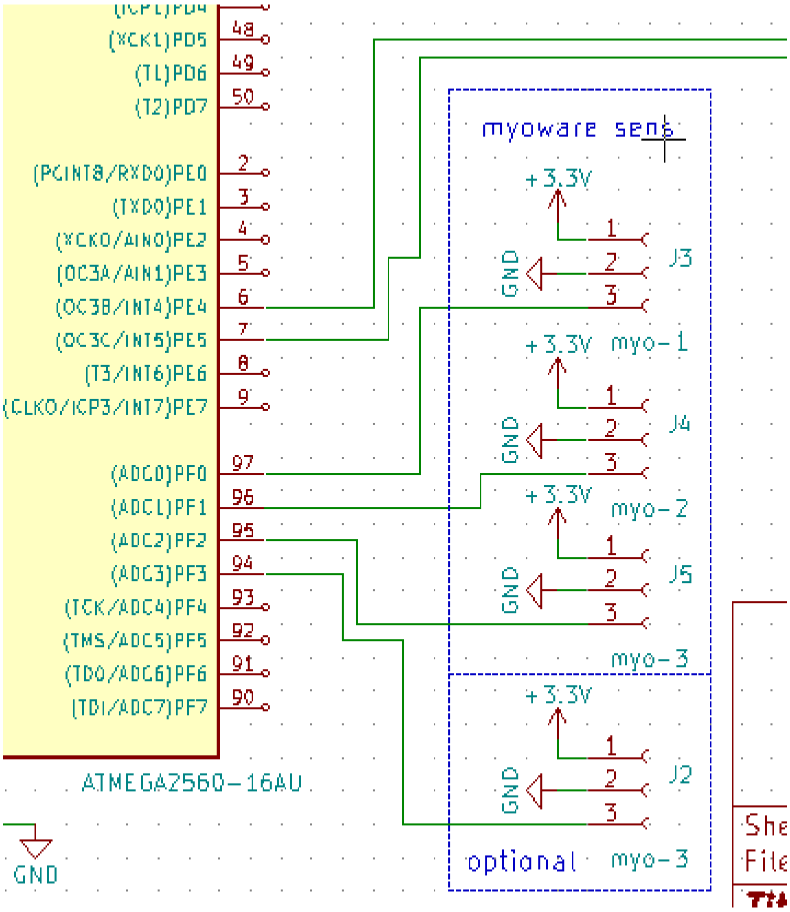


Figure 25: Myoware Muscle sensors' pin configuration.

## 4.3 DC Motor Driver Circuit

For finger actuation, a SG90 servo motor was chosen. This small and simple motor was chosen since it can provide the necessary features such as small size, light weight, integrated gearbox and cheap price. Despite all the advantages, this servo motor also has some limitations that were necessary to modify. SG90 are originally designed for a specific degree rotation, in this case it is 180 degrees and 90 degrees in each direction. This feature was caused by the hardware limit in gearbox and feedback potentiometer [18]. In this project, the servo motors need to be continuous rotation and continuous rotation feedback loop. Therefore, the motor's original feedback potentiometer chip was replaced by a H-bridge motor driver IC.

In general, the H-bridge is a rather simple circuit, containing four switching elements, with the load at the center. Figure 26 demonstrates an H-bridge motor driver configuration.

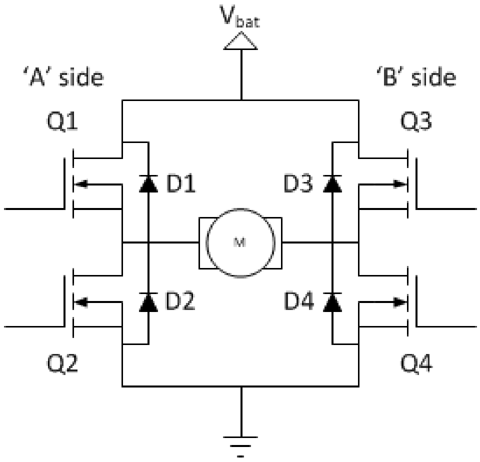


Figure 26: H-bridge motor driver configuration [23]

The basic operating principle of an H-bridge is fairly simple. According to above figure, if Q1 and Q4 MOSFET are turned on, the left lead of the motor will be connected to the power supply, while the right lead is connected to ground which will make the current starts flowing through the motor and energizes it. On the other hand, if Q2 and Q3 are turned on, the motor gets energized in the reverse direction, and the shaft will start spinning backwards.

The ZXBM5210 motor driver IC was chosen to control the SG90 DC motors in this project. The ZXBM5120 is a single chip solution for driving a single-coil reversible direct current (DC) fans or motors. This minimizes audible switching noise and electromagnetic interference (EMI) and provides a low noise solution by the integrated full bridge driver output stage inside. The chip has wide operating range voltage from 3 V to 18 V and internal over current and voltage protection. The ZXBM5120 has four different operations modes: Forward, Reverse, Break and Standby and the four modes are controlled by the FWD and REV login pins. Figure 27 demonstrates the four operation modes of the ZXBM5120 chip. [24]

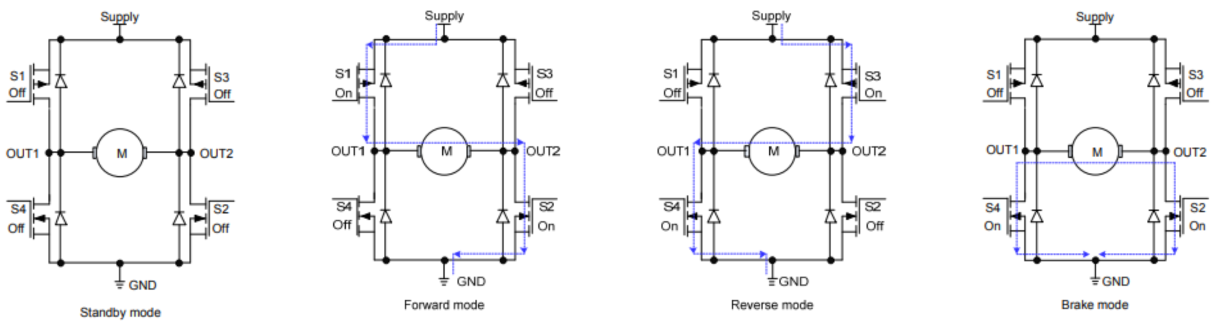


Figure 27: The ZXBM5120 operation mode. [23]

In total, the design has five DC motors to control each finger separately; therefore, five ZXBM512 was included in the circuit. Figure 28 shows the schematics design of the DC motor driver chip.

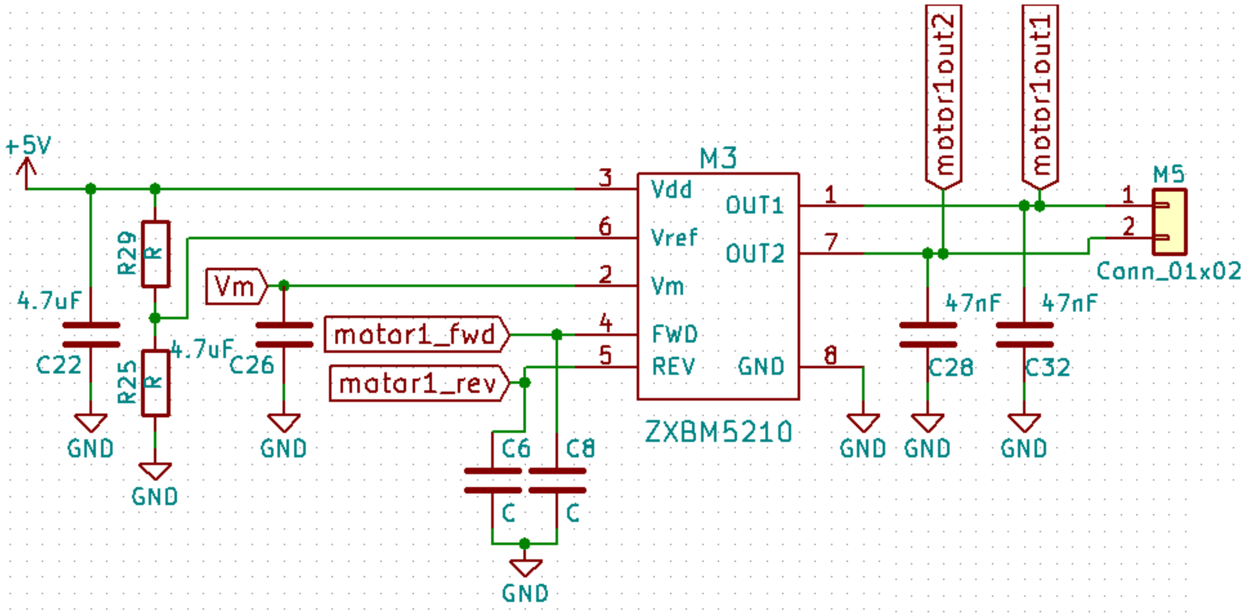


Figure 28: The DC motor drive schematic.

## 4.4 Power Management Circuit

The power management circuit consists of four main parts: power source, battery charger, boost converter and linear regulator. Most of the components work with 5 V power supply except the EMG sensors have 3.3 V power supply. The primary power source of the device is the rechargeable Li-ion battery; however, when there is no battery or the battery is out of charge the device can also be powered by external power source via micro B USB connector.

The circuit has been designed to be powered from one or more 3.7 V rechargeable Li-ion battery. Connecting multiple batteries in parallel helps to achieve higher energy and longer discharger time. The user can easily recharge the battery by connecting the device with external power source via micro USB connector. Figure 29 shows the recharge battery schematic.

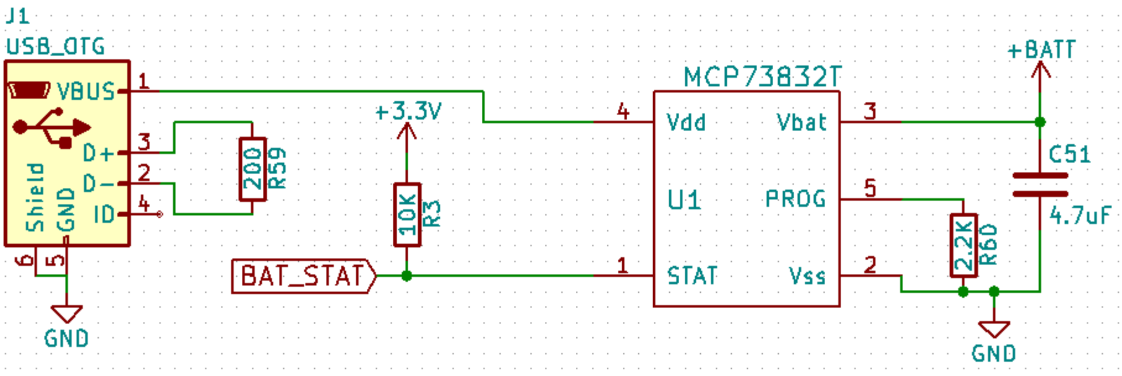


Figure 29: The recharge battery schematic

According to figure 29, the MCP7382T IC is used as Li-ion charger management controller. This integrated circuit was chosen because of its ability to provide many different feature in one single package such as small physical size, low number of external components, charging from USB port, constant current/voltage charge algorithm with selectable preconditioning and charge termination, fixed voltage and thermal regulation and automatic power-down function [25]. One of the most useful feature of this IC is charging from USB port since nowadays almost everybody has a mobile phone which is charged with USB port. Therefore, including the same standard USB connector in a circuit ensures that prosthesis user easily recharges the battery anywhere.

As shown in figure 29, the charging current is set by connecting the PROG pin with the Vss on the MCP73832T chip. The prefered fast charge current for Lithium-Ion cells is at 1 C rate, with an absolute maximum current at 2 C rate. For example, a 500 mAh battery pack has a preferred fast charge current of 500 mA. Charging at this rate provides the shortest charge cycle times without degradation to the battery pack performance or life. In contrast, the USB 2.0 standard is capable of supplying up to 500 mA of current; therefore, to avoid drawing too much current from appliances, the charging current has been calculated to be under 500 mA. The rechargeable current is calculated by the formula.

$$I_{reg} = 1000\frac{V}{Rprog} \quad (1)$$

Ireg: The rechargeable current

V: Power supply voltage from USB connector

Rprog: The value of the resistor that connected between PROG and Vss pin.

For this project, the target recharge current is around 450 mA. Base on the above formula, the Rprog is 2222 Ω; therefore, the closest standard resistor 2.2 kΩ was chosen to connect between PROG and Vss pin.

Most of the components in the circuit needs 5 V power supply; however, the output voltage of the battery is only 3.7 V. Therefore, a boost converter circuit is necessary to boost the output voltage of battery from 3.7 V to 5 V. As shown in figure 30, a boost simplification converter circuit.

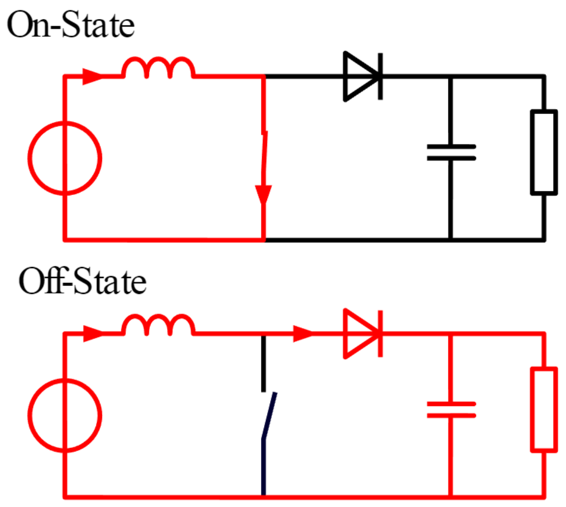


Figure 30: Boost simplification converter circuit [26]

The working principle of a boost converter can be divided into two modes (1 and 2). Mode 1 starts when the switch M1 is ON at time t = 0 and the current flows through the inductor L from left to right direction and the inductor stores some energy. The left side of the inductor L has positive polarity. Mode 2 starts when switch M1 is off at time t=t1, the current will be reduced as the impedance is higher. The inductor L polarity will be reversed. Hence, two sources will be in series causing a higher voltage to charge the capacitor through the diode D.

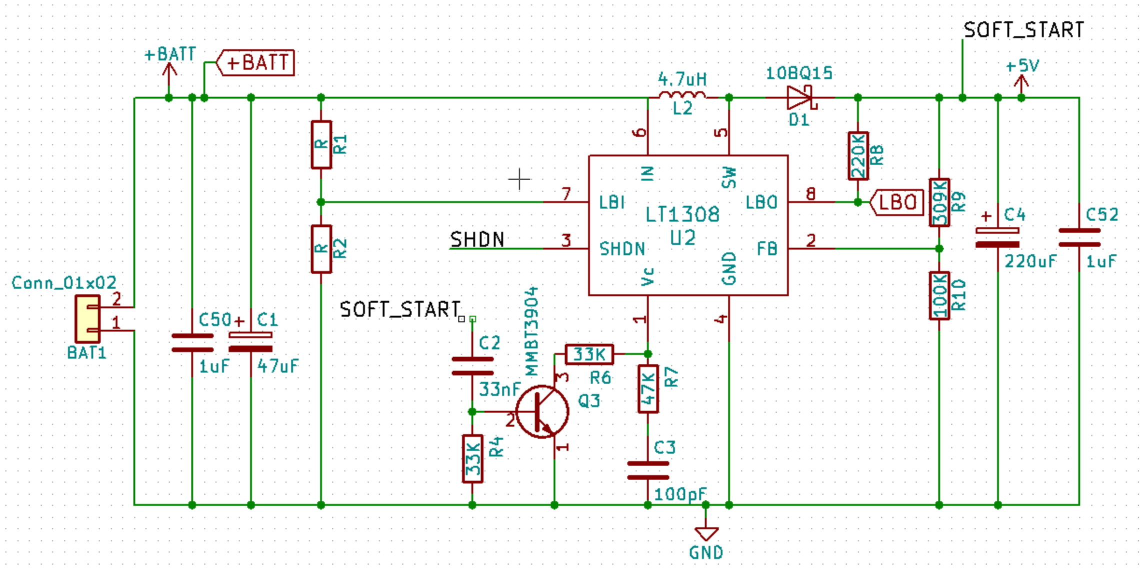


Figure 31: The boost converter schematic.

As shown in the figure 31, LT1308 boost converter chip was chosen in the design for this project because it is  a fixed frequency step-up DC/DC converters that operate over a 1 V to 10 V input voltage. This IC also has many useful features such as starts into heavy low, low quiescent current in shutdown (1 µA) and low-battery detector. According to figure 32, output voltage is set by using a resistor to create voltage divider to LBI which is connected to the internal reference. When the input voltage in LBI pin is above reference, the LBO pin will be pulled to a low state level. On the other hand, when LBI voltage drops below reference, the LBO pin will be pulled to high state level. The LBO level is readed by the microcontroller which helps to notify the user when the battery is low.

The boost converter’s output voltage is calculated by the below formula.

$$V_{out} = 1.22(1 + \frac{R_9}{R_{10}}) \qquad (2)$$

The R10 is chosen to be 100 kΩ and Vout needs to be 5 V. Based on the formula (2), the value of R9 can be calculated.

$$R_9 = R_{10}(\frac{V_{out}}{1.22} - 1) = 10^5(\frac{5}{1.22} - 1) = 309836[\Omega] \qquad (3)$$

According to R9 calculated value, the closest standard resistor is 309 kΩ and was chosen for the design.

## 4.5 Microcontroller Circuit

When all the components of the control system were determined, the microcontroller was chosen based on power requirement and number of inputs and outputs available. In total, the desired microcontroller needs at least twenty-eight digital, one PWM, nine analog pin to fulfill the requirement of the device. Thus, the ATMega2560 was chosen because it can not only provide enough input/output pin but also its ability to use a 16 MHz clock and power consumption is relatively low. Figure 32 demonstrates the microcontroller schematic.

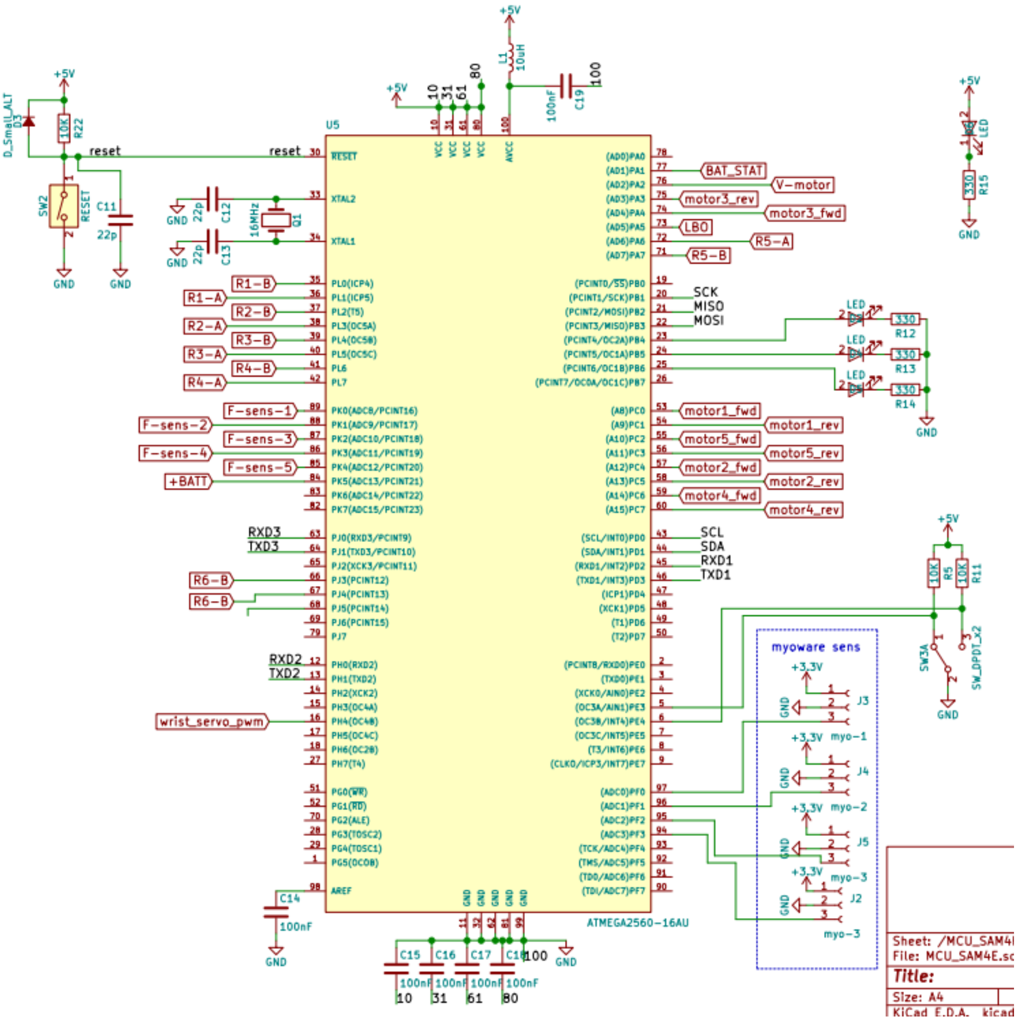


Figure 32: Microcontroller schematic

According to the figure 32, the bypass capacitors are applied between the power supply pins Vcc and GND of the IC. They reduced both the power noise and the result of spikes on the supply line. They also provide immediate current demands of the IC whenever it turns on. All the input analog and digital signal are connected the corresponding pin.

# 5 EMG Signal Processing

## 5.1 Myoware Sensor Attachment

When a muscle receives a neuromuscular signal from brain, it triggers an action potential in the muscle cell, it is basically just a voltage difference across the cell membrane. Surface electromyography techniques can be used to measure these voltages on the surface of skin. The measured electrical signal on skin surface can have varying frequencies depending on the strength of contraction of the muscle.

The EMG sensors were placed on different areas of forearm and biceps to read the electromyography signals. Since position and orientation of the muscle sensor electrodes has a vast effect on the strength of the signal, electrodes' places were carefully chosen by both theoretical anatomy of human muscle and empirical estimates. The electrodes should be place in the middle of the muscle body and should be aligned with the orientation of the muscle fibers. Placing the sensor in other locations will reduce the strength and quality of the sensor's signal due to a reduction of the number of motor units measure and interference attributed to crosstalk [22]. Figure 33 shows the comparison of raw EMG output when placing the electrode in different position.

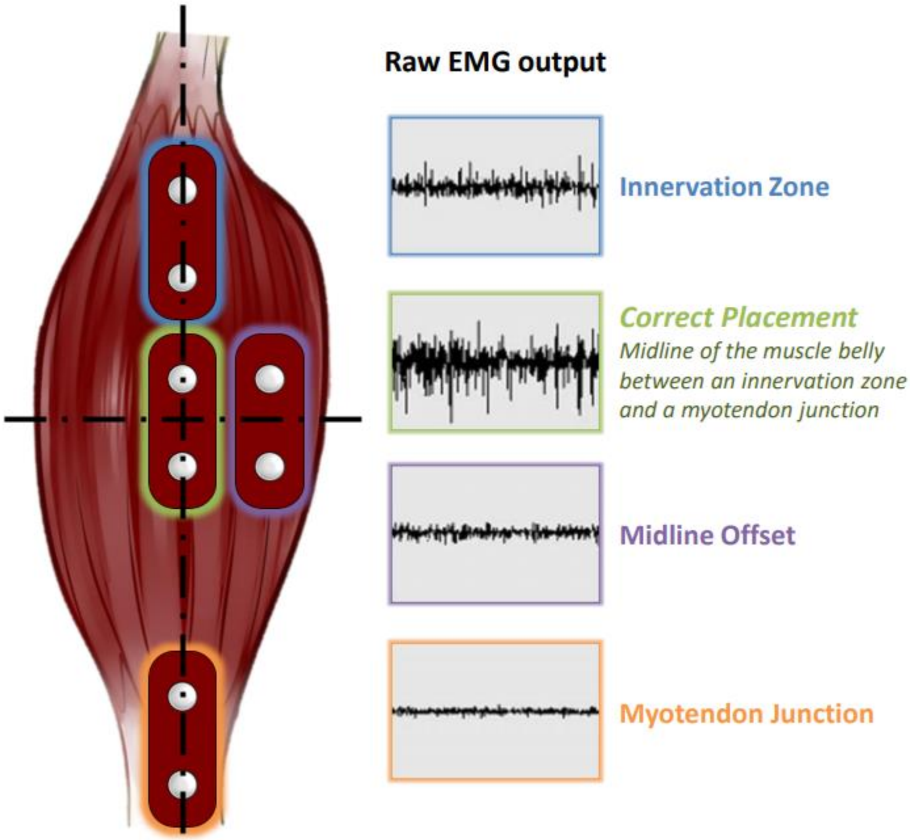


Figure 33: Raw EMG output when placing the electrode in different positions. [22]

In total, there are three MyoWare sensors which were placed on different areas of the user's forearm and biceps to read the electromyography signals. In order to differentiate the signals between the fingers and grip selection, two EMG sensors were placed on the forearm. One of them was placed on the underside of forearm to measure the EMG signal of the flexor digitorum muscle. The other one was set on the upperside of forearm to measure the signal of the extensor digitorum muscle. Another additional sensor was placed on the short head bicep muscle to control the prosthesis' wrist motion. The electrodes which were placed on underside, upperside forearm and on the biceps are labeled 1, 2 and 3 respectively. Figure 34 demonstrates all the EMG sensors' placement.

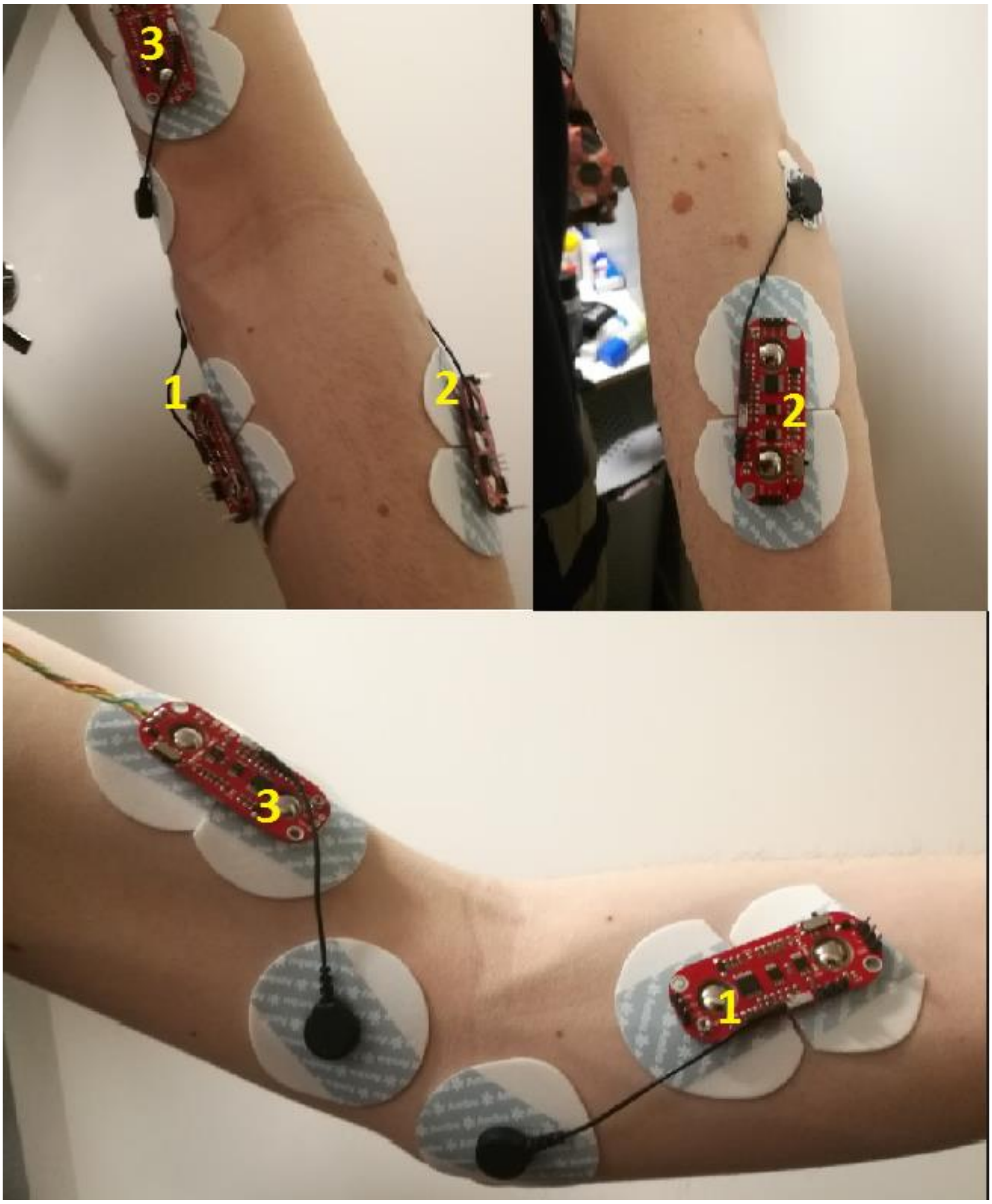


Figure 34: The EMG sensors' placement.

For this project, the Ambu WhiteSensor 4500M-H electrode pad was chosen because not only the electrode material is Silver Chloride (AgCl) but also it has a wet/conductive gel with good adhesion to ensure a good signal quality during measurement. The WhiteSensor electrode conductive gel contains Chloride ions. When a muscle in the vicinity of an electrode fires an action potential, it can be detected as a current of chloride ions on the skin. The chloride ions bind to a Silver atom and free an electron from the atom. The electron can then travel through a wire connected to the electrode as a normal current.

## 5.2 EMG Signal Processing Method and Algorithm

The raw EMG signal strength is very weak (~2 mV) and noisy. To improve the signal quality, the signal needs to be amplified, rectified and filtered carefully. Fortunately, the MyoWare sensor was designed to be used directly with a microcontroller. Therefore, the primary output of MyoWare sensor is not a RAW EMG signal but rather an amplified, rectified and integrated signal. The output signal from the sensor works well with a microcontroller analog to digital converter (ADC). Figure 35 illustrates the differences between raw, rectified and rectified and integrated signal. [22]

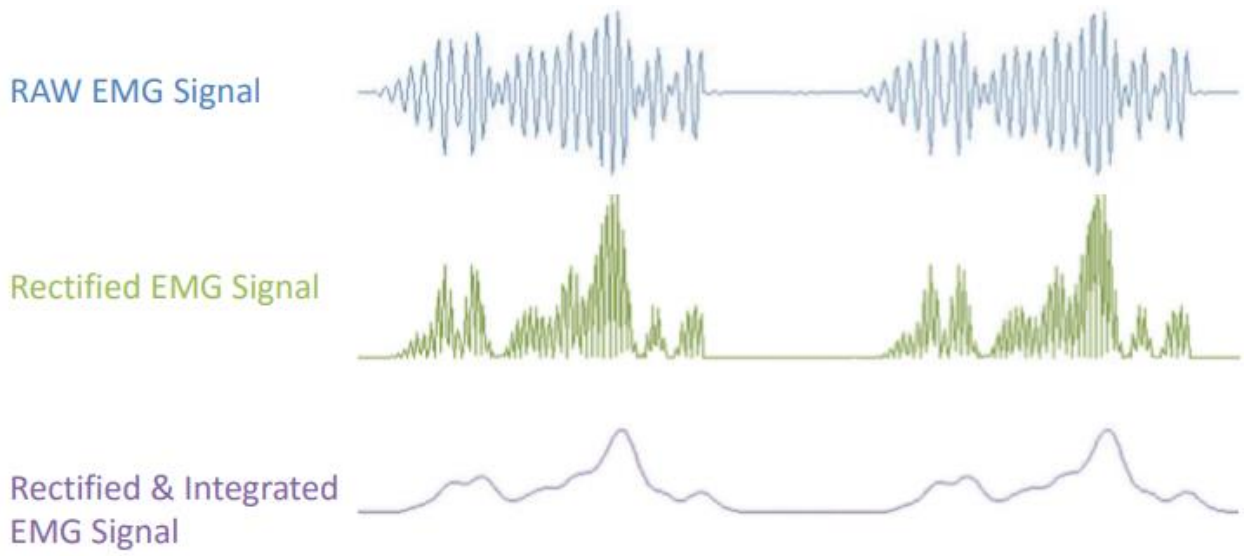


Figure 35: The differences between raw, rectified; and rectified and integrated signal.

Human real hand can perform hundreds of different gestures or poses thank to complicated bones, joints, muscles and nervous system. However, the outcome device of this project can only perform six different hand gestures such as rest, fist, wrist flexion, point, pinch and rock due to the limitation of software, hardware, time and budget. In order to control the prosthetic hand to perform different poses, the user just needs to remember and performs different sequences on the real hand. The device measures and classified the EMG signal from the MyoWare sensors which are attached on the user's forearm and bicep to distinguish between different poses of the user real hand. The fingers and wrist of the prosthetic hand are controlled base on the outcome of EMG signal classification function. The table 2 describes the real hand pose corresponding with the prosthetic hand pose. For example, when the users close their fist and make the wrist flexion the same time, the prosthetic hand will make point gesture (all four fingers close except index finger and when the user totally relax their muscle, the prosthetic hand will open all five finger and make the rest pose.

Table 2: Mapping gestures between the user real and prosthetic hand poses. [27]

| No. | The Real Hand Pose | Description | The Prosthetic Hand Pose | Description |
|---|---|---|---|---|
| 1. |  Fist | All five fingers closed |  Fist | All five fingers closed |
| 2 |  Fist and wrist flex-ion | All five fingers closed and wrist flexion |  Point | All four fingers closed except in-dex finger |
| 3 |  Wrist flexion | Wrist flexion |  Rock | All three fingers closed except in-dex and pinky fin-gers |
| 4 |  Wrist extension | Wrist exten-sion |  Pinch | All three fingers closed except ring and pinky fin-gers |
| 5 |   Rest | All five fingers opened |  Rest | All five fingers opened |

| | | | | |
|---|---|---|---|---|
| 6 |  Bicep | Bicep muscle tightens |  Wrist flexion | Wrist moves up to 50 degrees from rest position. |

The quality of the output data from MyoWare sensors is fairly good already but the filtering incoming signal from sensor is still necessary to accurately predict the user's desired action. The moving average and Kalman filter are used to filter the incoming data which is then sent to the data clustering algorithm to accurately determine the user's input. Figure 36 shows the flowchart of data processing procedure.

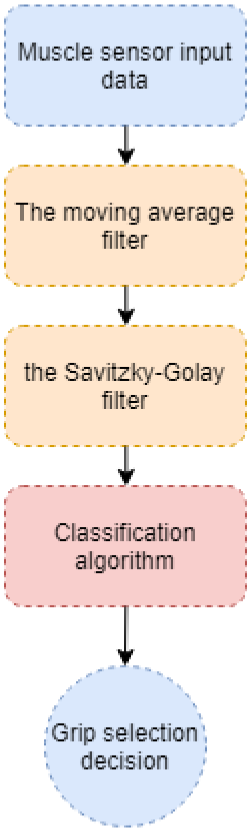


Figure 36: The flowchart of data processing procedure.

The first stage of data processing cycle is data filter. The signal from EMG sensors is inherently noisy, because of this, predicting the user's actions is more difficult at a single point in time. One of the ways to solve this problem is through filtering the stream of data. As such, a moving average and Steady-State and Transient Savitzky-Golay Filters were implemented as a software filter for this purpose.

The moving average filter is a simple Low Pass FIR (Finite Impulse Response) filter commonly used for smoothing an array of sampled data/signals [28]. This filter simply takes N samples of input at a time and take the average of those N-samples and produces a single output point. The moving average of streaming data is computed with a finite sliding window:

$$movAvg = \frac{x[n] + x[n-1] + ... + x[n-N]}{N+1} \quad (4)$$

N+1 is the length of the filter.

The Steady-State and Transient Savitzky-Golay Filter is a digital filter that is used to smoothing a set of digital data points to increase the signal-to-noise ratio without greatly distorting the signal. This filter fits successive subsets of adjacent data points with a low-degree polynomial by the method of linear least squares [29].

Assuming that filter length or frame size N is odd, N = 2M+1 and N >= d+1, where d = polynomial order.

$x_n$: The noisy sample, n = 0, 1,..., L-1

$y_n$: The smoothed output result, n = 0, 1,....,L-1

Data vector x have n = L input points and x = $[x_0, x_1, ....., x_{L-1}]^T$ is replaced by N dimensional one, having M points of each side of x: x = $[x_M, \ldots, x_1, x_0, x_1, \ldots, x_M]^T$

If n >= L-1-M, the output result of Steady-State and Transient Savitzky-Golay Filter is calculated by formula:

$$y_{L-1-M+m} = b^T_{-m} w(L-1-M) \quad (5)$$

m = 0, 1...., M where

$$w(L-1-M) = \begin{bmatrix} x_{L-1} \\ x_{L-2} \\ . \\ . \\ x_{L-N} \end{bmatrix} \quad (6)$$

As seen in figure 37, the moving average and Steady-State and Transient Savitzky-Golay Filters smooth the data quite well.

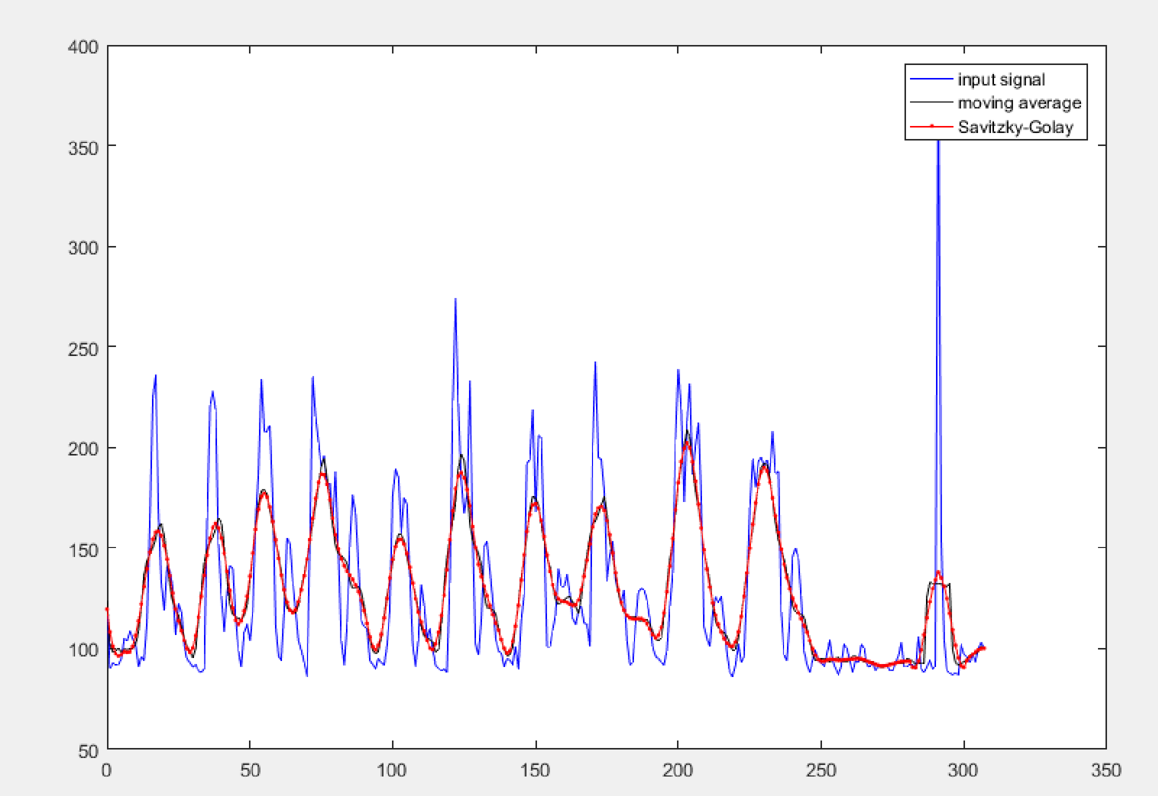


Figure 37: Moving Average and Savitzky-Golay on Muscle Sensor data.

Once run through all the filters, the data is then analyzed to estimate the threshold of the data base on the calibration result when muscle is totally relaxed. When the muscle is totally relaxed, the microcontroller calculates the maximum value of the EMG signal and set it as the threshold to distinguish between relaxed and flexed stage of muscles. Figure 38 shows how the threshold has been set.

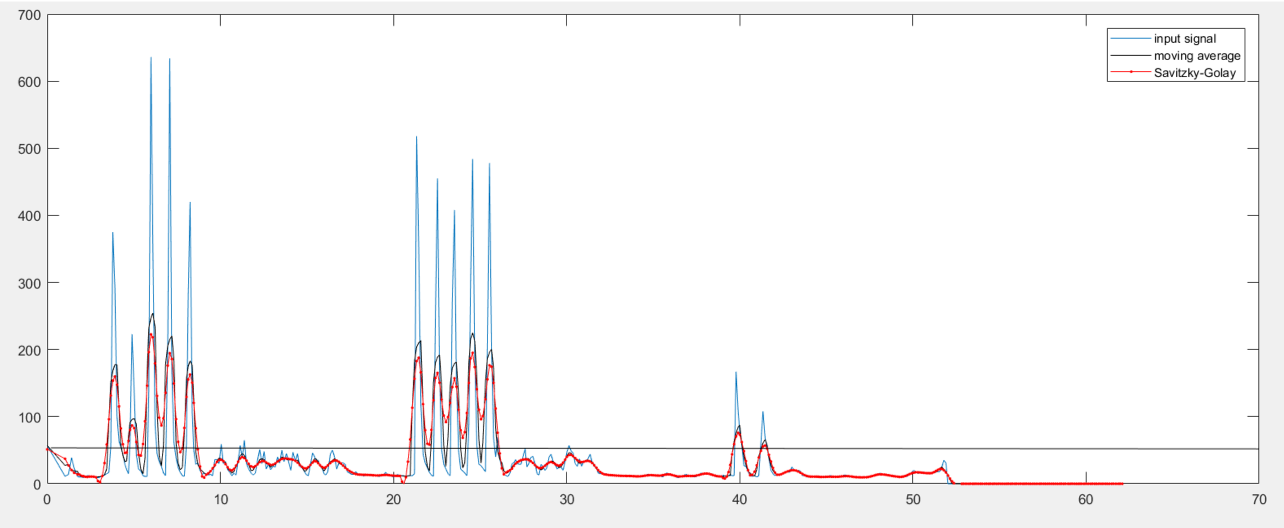


Figure 38: The EMG signal threshold

Based on the flexed and relaxed status of all three sensor, the devices can classify the signal of six different poses: rest, fist, fist and wrist flexion, wrist flexion, wrist extension and bicep flexed. For example, when the user's hand forms a fist, the sensor which are attached on upperside and underside forearm are activated but the sensor on bicep is inactivated. In the rest pose, none of the sensors are activated. Table 3 shows each sensors status with different real hand gestures.

Table 3: Sensors status with different real hand gestures.

| No. | The Real Hand Pose | Sensors status |
|---|---|---|
| 1. |  Fist | • Upperside forearm: activated<br>• Underside forearm: activated<br>• Bicep: inactivated |
| 2 |  Fist and wrist flexion | • Upperside forearm: activated<br>• Underside forearm: activated<br>• Bicep: activated |
| 3 |  Wrist flexion | • Upperside forearm: inactivated<br>• Underside forearm: activated<br>• Bicep: inactivated |
| 4 |  Wrist extension | • Upperside forearm: activated<br>• Underside forearm: inactivated<br>• Bicep: inactivated |
| 5 |   Rest | • Upperside forearm: inactivated<br>• Underside forearm: inactivated<br>• Bicep: inactivated |

| | | |
|---|---|---|
| 6 |  Bicep | • Upperside forearm: inactivated<br>• Underside forearm: inactivated<br>• Bicep: activated |

## 6 Firmware coding

There are two different modes which are calibration and operation mode. The users can easily switch between two modes by pressing on the latch button including on the PCB. The main purpose of calibration mode is to measure the signal and calculate the threshold to classify when the measurement muscle is flexed and relaxed. At the beginning of calibration mode, the system will spend around 15 seconds to measure the EMG signal when all the muscles are totally relaxed, three yellow, red and blue LEDs blink in turn until the end of the process. After this stage, the system can determine the maximum filtered EMG value when the muscles are relaxed and set the threshold for each separate sensor. After the first stage, the users need to perform all six hand gestures each of them four times in an arranged order: fist and wrist flexion, fist, wrist flexion, wrist extension and flexed bicep. The users need to flex the corresponding muscle when the yellow LED is on the PCB is turn on and relax them when the LED turn off. The action continues until all the hand gestures has been carefully tested. The result of each test case is a three element Booleans array which will be compared with the reference matrix of hand gesture classification. Figure 39 shows reference array of classification method.

```
bool reference_array [6][3] = {{1, 1, 1},          //Fist and wrist flexion
                               {1, 1, 0},          //Fist
                               {0, 1, 0},          //Wrist flexion
                               {1, 0, 0},          //Wrist extension
                               {0, 0, 1},          //Bicep flexed
                               {0, 0, 0}};         //Rest
```

Figure 39: Reference array of classification method.

When the calibration mode has been done and the threshold has been measured and calculated, the user can press the latch button to switch to operation mode. At the beginning of operation mode, the EMG signal is collected and based on that the system uses the classification method to determine the right grip selection to control the prosthetic hand. Based on the grip selection output, the corresponding motors actuate. During the closing state, the force sensor readings are used to determine whether an object is either blocking or in the grasp of a finger and that finger should stop moving. In general, the movement of motors were programed in the way that each of them has a maximum of 6 degrees further towards its deserve state from the previous state until the finger's respective force sensor reaches its threshold reading or the finger reaches its desired position. In order to make the motors operate accurately, rotary encoder reading method is very important. The rotary encoder that was used for this project has two input A and B. When the rotary rotates, there is phase shifted square wave signal on the both outputs. One of the method to read rotary encoder is 2-bit gray code. As shown in figure 41, when the encoder rotates clockwise direction, the outputs' gray code is 2->3->1->0->2 and so on. On the other hand, when it rotates counter-clock wise, the sequence will be 3->2->0->1. Figure 40 shows the outputs' gray code when the rotary encoder rotates clockwise (CW) and counter-clockwise (CCW). [29]

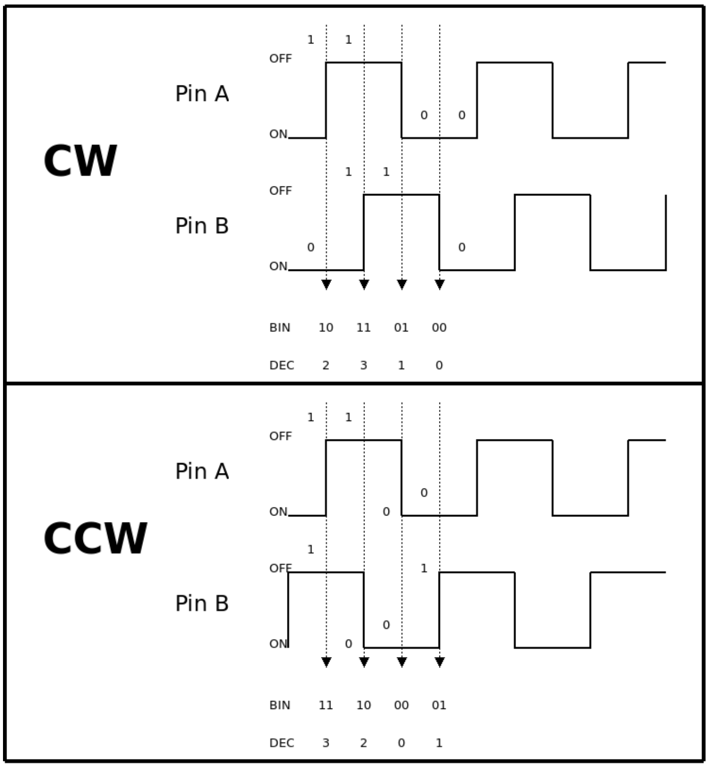


Figure 40: Gray code rotary encoder [29]

When the motors stop rotating, a Boolean variable is set to state that the finger is finished moving. In addition, with different hand gesture, the user can also control the wrist movement by only activating the sensor which is attached on bicep. If the bicep sensor is activated and the wrist state is down, the PWM motor is the wrist will move up around 50 degrees. At the end of the cycle all the motors are released back to hand rest position and start the new loop iteration after that. Figure 41 and 42 illustrates that logic flow chart and operation mode chart respectively.

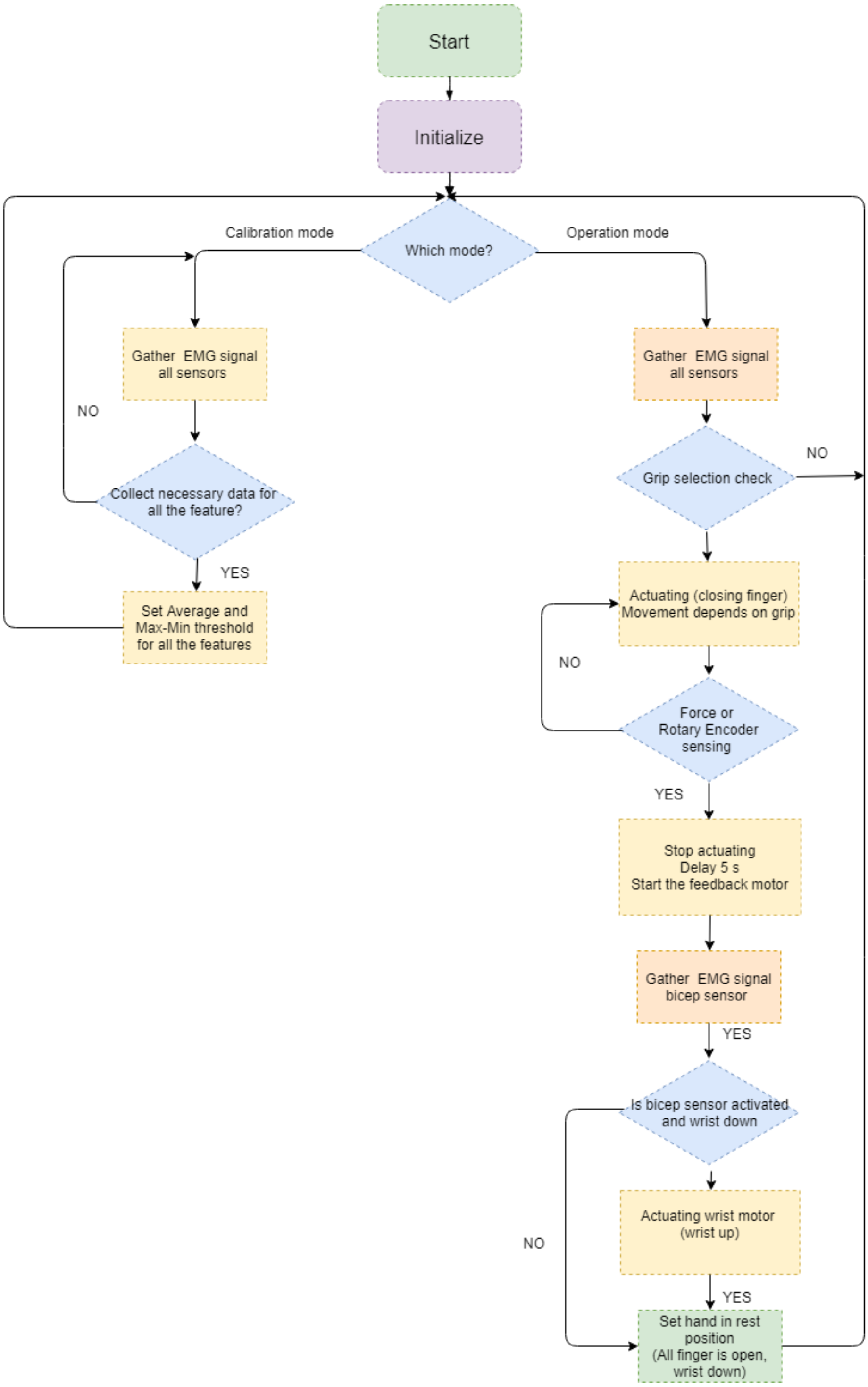


Figure 41: Logic Flow Chart

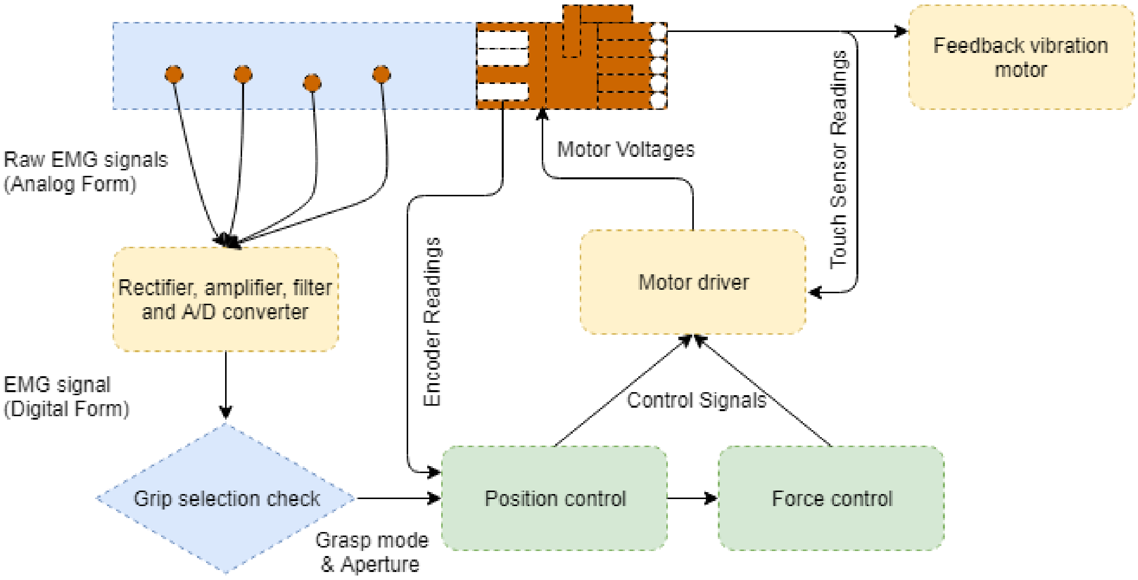


Figure 42: Operation Mode Chart

# 7 Costs

One of the main goals of this project is to develop a low-cost prosthetic hand for the patients in the developing countries. Therefore, the device cost estimation is extremely important. This chapter focuses on the device cost breakdown and the cost prediction in the future. According to table 4, the final price of the product is around 190 € which is much cheaper compared to all the other available electronics prosthetic hand in market. Normally a commercial prosthetic hand would cost couple thousands of euros, for example, the Bebionic hand of Ottobock Ltd. The most expensive components in the whole product is three MyoWare Muscle sensors which take up to 50% of the total cost. The price of the final product can be reduced around 16% by applying better EMG signal processing method and eliminating one MyoWare Muscle sensor.

Table 4: The device cost by part

| Description | Vendor | Cost/Unit (€) | Quantity | Total cost (€) |
|---|---|---|---|---|
| PCB board | | 8.4 | 1 | 8.4 |
| MyoWare Muscle sensor | Mouser | 30.53 | 3 | 91.59 |
| Force sensor | Mouser | 5.532 | 5 | 27.66 |
| LT1308BCS8 | Mouser | 5.4 | 1 | 5.4 |

| | | | | |
|---|---|---|---|---|
| SG90 motor | Aliexpress | 1.34 | 5 | 6.7 |
| MG996R big servo motor | Aliexpress | 4.08 | 1 | 4.08 |
| MCP73832 | Mouser | 0.48 | 1 | 0.48 |
| ATMega 2560 16AU | Mouser | 10.3 | 1 | 10.3 |
| ZXBM5210<br>Motor driver | Mouser | 0.81 | 5 | 4.05 |
| P15965CT-ND<br>Rotary encoder | Mouser | 1.48 | 5 | 7.4 |
| Resistor | Mouser | 0.01 | 30 | 0.3 |
| Capacitor | Mouser | 0.01 | 20 | 0.2 |
| Filament | Clas Ohlson | 25 | 0.3 | 7.5 |
| Other | Mouser | N/A | N/A | 15 |
| | | | Total | 189.06 |

## 8 Conclusion and future improvement

For an amputee, upper limbs loss has many different consequences. Due to the hand loss, the number of work and life opportunities is greatly reduced for them. Hence, research into creating a prosthetic hand which can be conveniently controlled by EMG signal from arm is of great value. Therefore, the goal of this project was to create a low-cost 3D printed prosthetic hand by using Electromyography data collected from the forearm.

The design partly met the project's expectation and goals set at the beginning. Initially, this project has four main targets. The first target is building a device in the form of a prosthetic hand which can help an upper limb loss amputee perform simple daily tasks. The device can only partly fulfil this target, because all the EMG signal measurement of different hand gestures were conducted on a person who does not loss his/her hand. In reality, the muscle group activities and EMG signal of an amputee may significantly differ from the one who still has a hand. There is a high probability that the device will not operate correctly when the user is an amputee. Secondly, the size needs to be adjustable and the weight needs to be light. The total weight of the device is around 412 grams which a really low and suitable for most of the users. However, the current mechanics design of the device does not allow the size to be adjustable, there are some new design updates planned for the future. Thirdly, the device should help the patients to “feel” the signal from the touch sensors. This target was achieved through the use of a vibration motor which is attached to the patient forearm. Whenever any of the forces sensors are activated, the vibration motor will be turned on to give the notification for the user about the grip’s force. Finally, the price needs to be cheaper than the other commercial products in the market. In fact, the final price of the device is only around 190 € which is much cheaper compared to most of the other available electronics prosthetic which can be cost thousands of euros such as Bebionic of Ottobock Ltd.

Although the final device has fulfilled most of the initial targets, there are many details of the current model that need to be redesigned in order to use it for real-life cases. Firstly, it is possible to save the device’s weight up to 20% by using carbon fiber filament and choosing another internal filling structure technique. Secondly, the flexible filament that was used to create the prosthetic hand joints is not flexible enough to return the hand in rest position after the movement, another flexible material needs to be chosen to replace the current one. Thirdly, the wire management is this model has been badly done, the wires are placed everywhere in the gauntlet of the hand. This problem can be solved by replacing the wire with ribbon cable of flat flex PCB and the connection to the PCB board should be made by a single line connector instead of many connectors distributed across the PCB. Finally, the EMG data signal processing needs to be studied and applied for the device in order to eliminate the calibration mode since the calibration mode brings a lot of inconveniences for the user at the moment.

## References

[1] https://tspace.library.utoronto.ca/bitstream/1807/11710/1/MQ28865.pdf

[2]https://pdfs.seman-ticscholar.org/3492/466936e797a0a834f094cc01cb3f607425c7.pdf

[3] https://www.bodybuilding.com/fun/how-to-build-monster-forearms.html

[4] Reinis Geizans, Developing 3D printed prosthetic hand model controlled by EMG signal from forearm

[5] Herberts, P., Almstrom,C., Caine, K., Clinical Application Study of Multifunctional Prosthetic Hands, Journal of Bone and Joint Surgery, Vol. 60B:p.552-560, 1978

[6] Hollister, A., Giurintano, D., How Joints Move, Clinical Mechanics of the Hand, 2nd. Edition (Brand, P., Hollister, A., edt), Mosby - Year Book Inc., St. Louis, Baltimore 1993

[7] Taylor, C.L., Schwarz R.J., The Anatomy and Mechanics of Human Hand, Artificial Limbs 2(2):pp.22-25, 1955

[8] https://www.researchgate.net/figure/Human-hand-skeletal-structure-depicting-finger-bones-joints-metacarpals-and-carpal_fig2_318184055

[9] https://hr.wiktionary.org/wiki/hand

[10] http://teachmeanatomy.info/upper-limb/muscles/posterior-forearm/

[11] https://corewalking.com/muscles-fingers/

[12] Delph, M.A., II, Fischer, S.A., Gauthier, P.W., & Martinez Luna, C.H., Rehabilitative Robotic Glove (Rep.). Retrieved September 25, 2016, from WPI Automation and Inter-ventional Medicine Laboratory. Website: https://web.wpi.edu/Pubs/E-project/Available/E-project-042512-143542/unre-stricted/Rehabilitative_Robotic_Glove_MQP.pdf

[13] http://bebionic.com/the_hand/technical_information/

[14] http://enablingthefuture.org

[15] Cameron Currie (BME/ME), A. Rae Nistler (ME), Cameron Downey (ME), David McDonald (ME), Gregory Port (RBE), Joseph Sabatino (ME), Steven Souto (ECE), De-sign and Development of a Myoelectric Transradial Prosthesis

[16] https://www.thingiverse.com/thing:380665

[17] https://3dprint.com/8122/flexy-hand-2-3d-printed-hand/

[18] https://www.velleman.eu/products/view/?id=43280

[19] http://www.ee.ic.ac.uk/pcheung/teaching/DE1_EE/stores/SG90_datasheet.pdf

[20] https://electronicsclub.info/blockdiagrams.htm

[21] https://www.sparkfun.com/products/13723

[22]https://cdn.sparkfun.com/datasheets/Sensors/Biometric/MyowareUserManualAT-04-001.pdf

[23] https://modularcircuits.com/blog/wp-content/uploads/2011/10/image8.png

[24] https://www.diodes.com/assets/Datasheets/ZXBM5210.pdf

[25] http://ww1.microchip.com/downloads/en/DeviceDoc/20001984g.pdf

[26] http://ethesis.nitrkl.ac.in/4811/1/109EE0612.pdf

[27] https://www.gaussianwaves.com/2010/11/moving-average-filter-ma-filter-2/

[28] https://en.wikipedia.org/wiki/Savitzky%E2%80%93Golay_filter

[29] http://www.leniwiec.org/en/2014/04/28/rotary-shaft-encoder-how-to-connect-it-and-handle-it-with-avr-atmega8-16-32-168-328/

## "Flexy Hand 2" part diagram

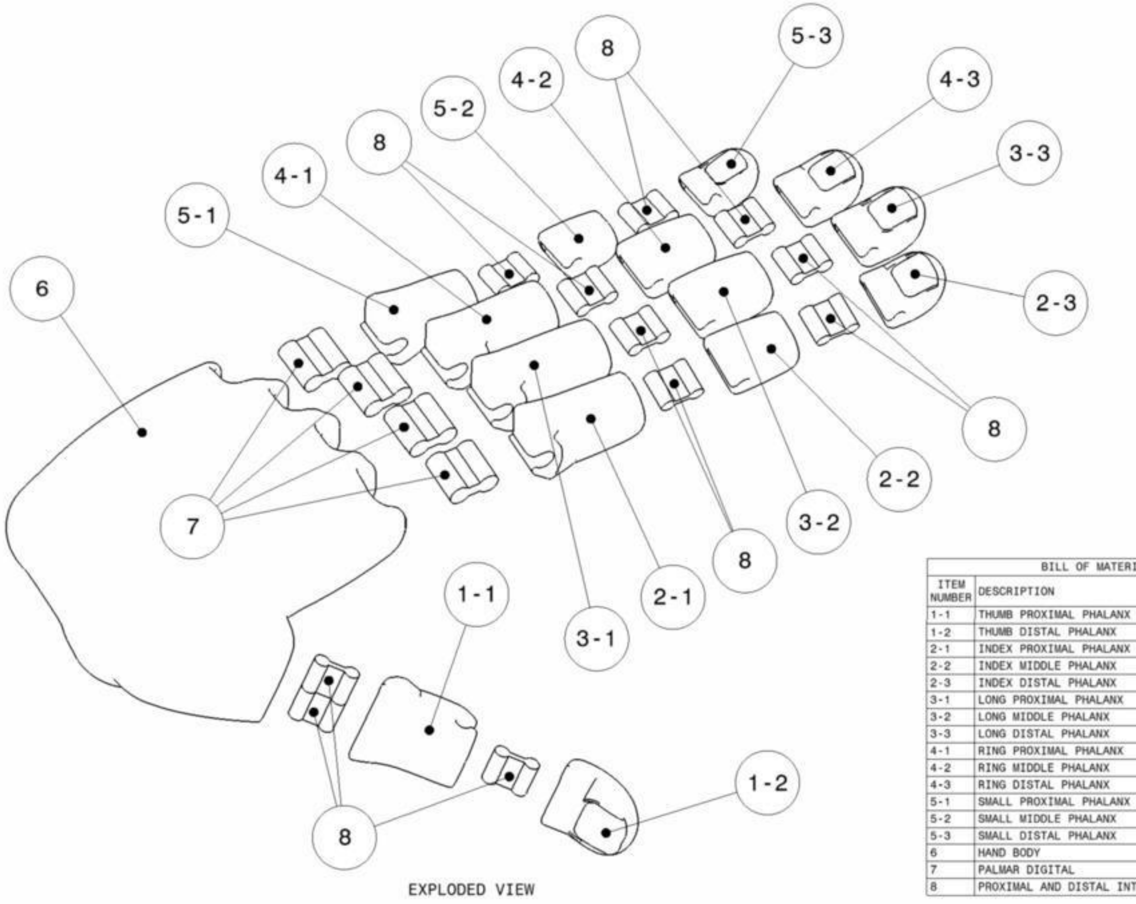


| BILL OF MATERIALS | | |
|---|---|---|
| ITEM NUMBER | DESCRIPTION | NUMBER OFF |
| 1-1 | THUMB PROXIMAL PHALANX | 1 |
| 1-2 | THUMB DISTAL PHALANX | 1 |
| 2-1 | INDEX PROXIMAL PHALANX | 1 |
| 2-2 | INDEX MIDDLE PHALANX | 1 |
| 2-3 | INDEX DISTAL PHALANX | 1 |
| 3-1 | LONG PROXIMAL PHALANX | 1 |
| 3-2 | LONG MIDDLE PHALANX | 1 |
| 3-3 | LONG DISTAL PHALANX | 1 |
| 4-1 | RING PROXIMAL PHALANX | 1 |
| 4-2 | RING MIDDLE PHALANX | 1 |
| 4-3 | RING DISTAL PHALANX | 1 |
| 5-1 | SMALL PROXIMAL PHALANX | 1 |
| 5-2 | SMALL MIDDLE PHALANX | 1 |
| 5-3 | SMALL DISTAL PHALANX | 1 |
| 6 | HAND BODY | 1 |
| 7 | PALMAR DIGITAL | 4 |
| 8 | PROXIMAL AND DISTAL INTERPHALANGEAL | 11 |

**"Flexy Hand 2"**

**part diagram**

## Schematic of the Myoelectric Prosthetic Hand

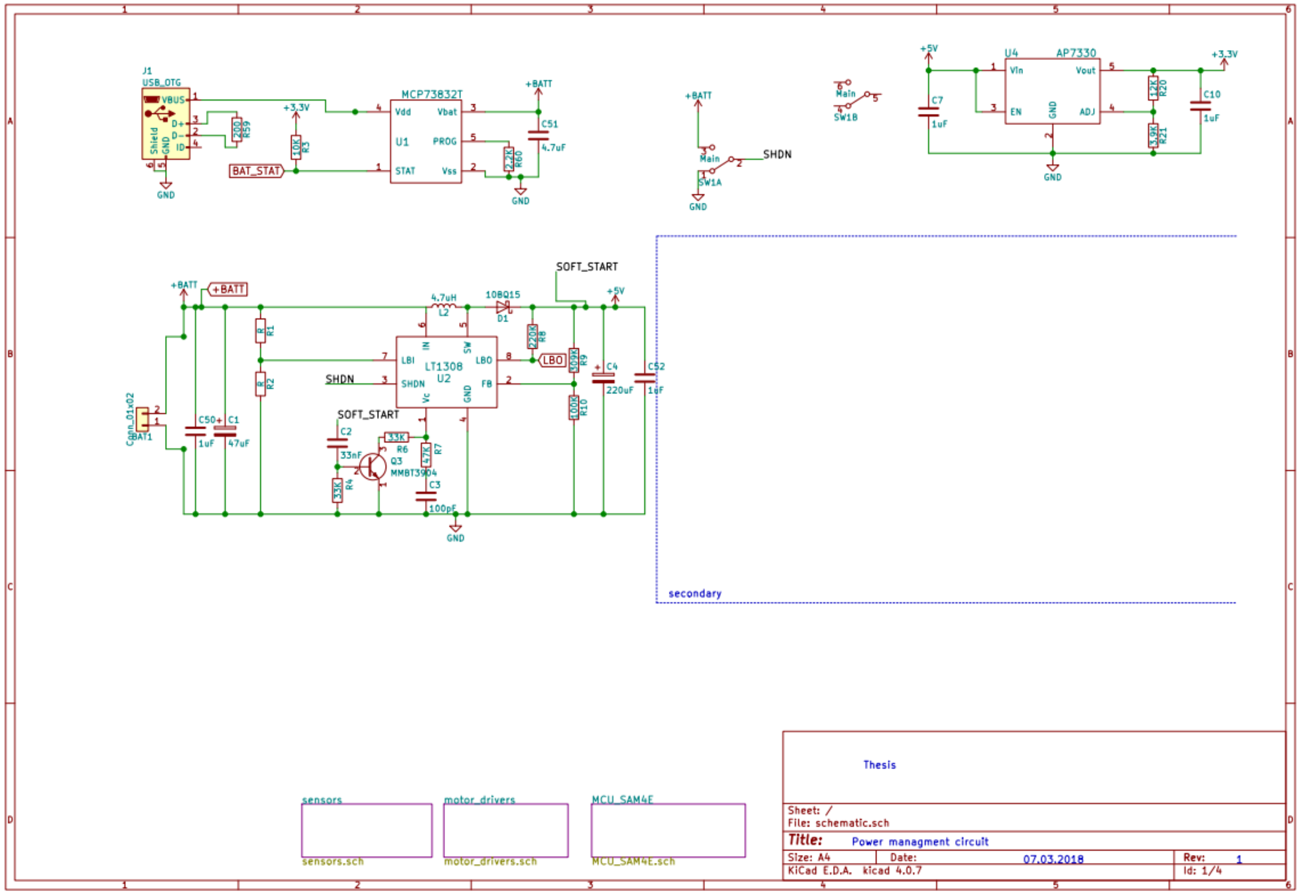


**Schematic of Power Management Circuit**

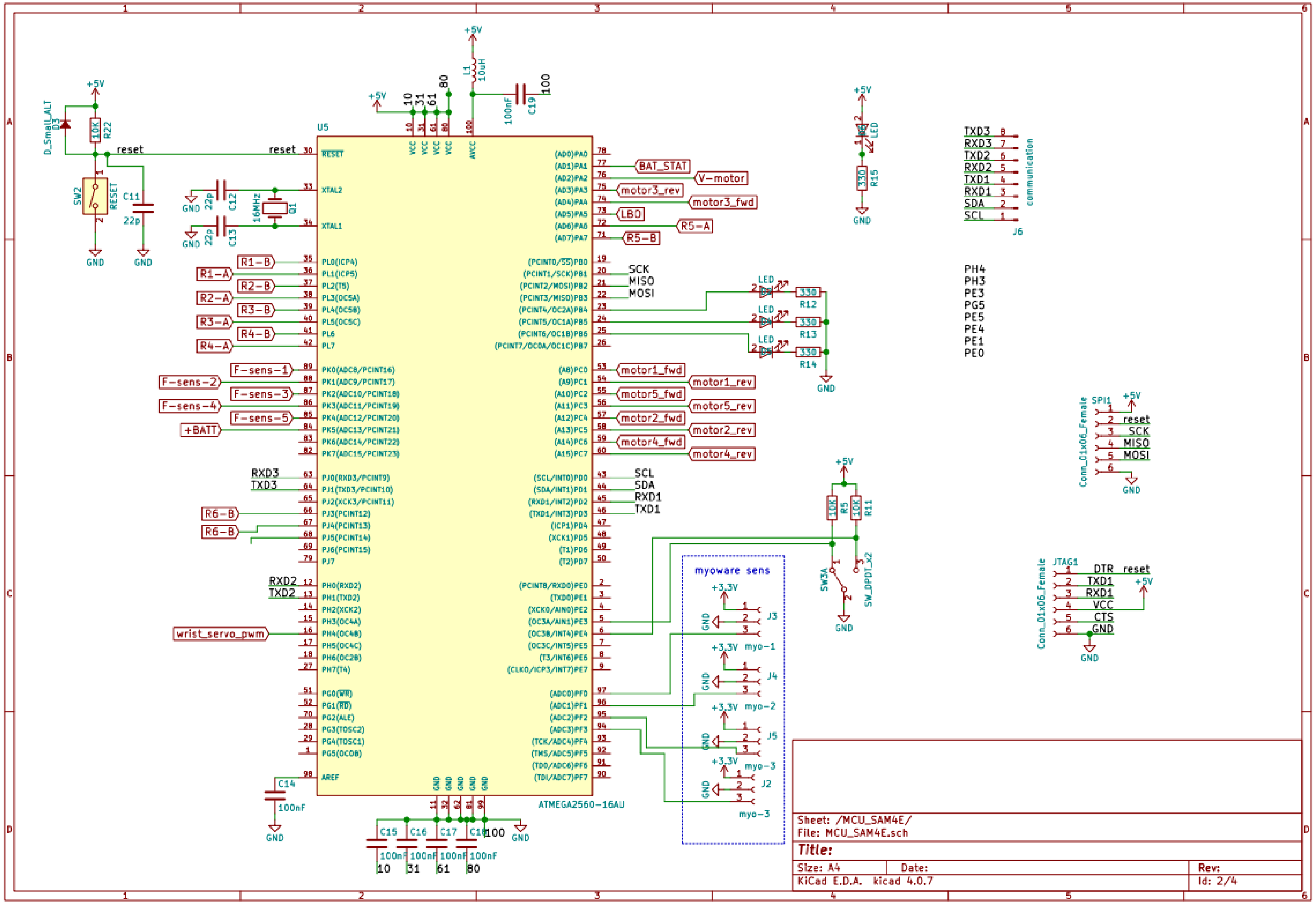


**Schematic of MCU circuit**

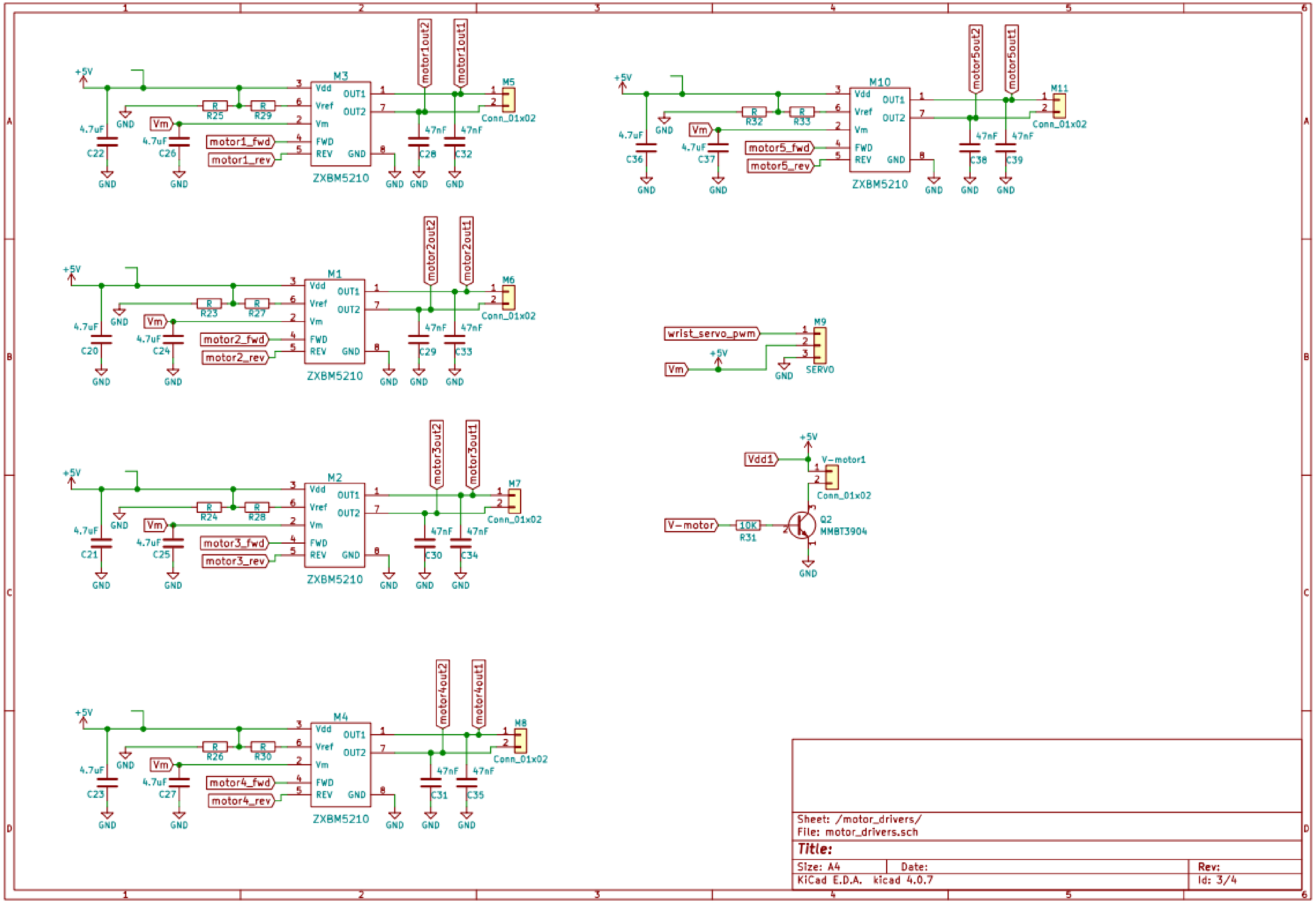


**Schematic of**

**Motor Control Circuit**

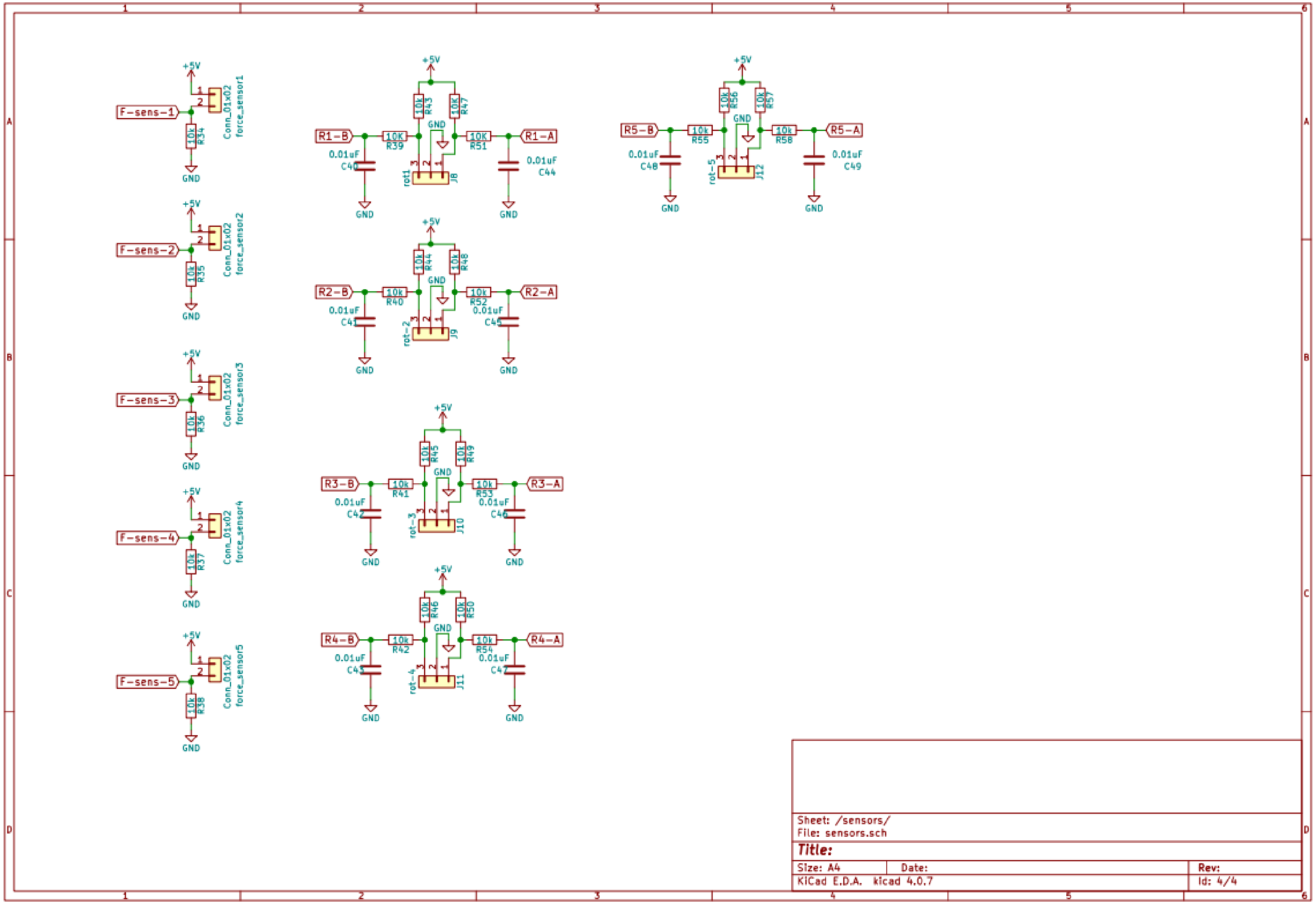


**Schematic of**

**Rotary Encoder Circuit**